Hindawi
Shock and Vibration
Volume 2018, Article ID 8759074, 22 pages
https://doi.org/10.1155/2018/8759074

Research Article

A Modified Fourier–Ritz Formulation for Vibration Analysis of Arbitrarily Restrained Rectangular Plate with Cutouts

Yiming Liu,[1] Zhuang Lin,[2] Hu Ding,[3] Guoyong Jin,[1] and Sensen Yan[1]

[1]*College of Power and Energy Engineering, Harbin Engineering University, Harbin 150001, China*
[2]*College of Shipbuilding Engineering, Harbin Engineering University, Harbin 150001, China*
[3]*Shanghai Marine Equipment Research Institute, Shanghai 200031, China*

Correspondence should be addressed to Zhuang Lin; 18845168688@163.com and Guoyong Jin; guoyongjin@hrbeu.edu.cn

Received 4 April 2018; Accepted 25 July 2018; Published 16 October 2018

Academic Editor: Lorenzo Dozio

A modified Fourier–Ritz method is developed for the flexural and in-plane vibration analysis of plates with two rectangular cutouts with arbitrary boundary conditions, aiming to provide a unified solving process for cases that the plate has various locations or sizes of cutout, and different kinds of boundary conditions. Under the current framework, modifying the position of the cutout or the boundary conditions of the plate is just as changing the geometric parameters of the plate, and there is no need to change the solution procedures. The arbitrary boundary conditions can be obtained by setting the stiffness constant of the boundary springs which are fixed uniformly along the edges of the plate at proper values. The strain and kinetic energy functions of a plate with rectangular cutout are derived in detail. The convergence and accuracy of the present method are demonstrated by comparing the present results with those obtained from the FEM software. In this paper, free in-plane and flexural vibration characteristics of the plate with rectangular cutout under general boundary conditions are studied. From the results, it can be found that the geometric parameters and positions of the cutout and the boundary conditions of the plate will obviously influence the natural vibration characteristics of the structures.

1. Introduction

As one of the most commonly used structures, the rectangular plate has been in study for a long time. It is well known that, in a vibrating thin plate, there exist three types of modes: bending mode, longitudinal mode, and shear mode. The bending mode is referred to the out-of-plane vibration, while the longitudinal mode and shear mode are referred to the in-plane vibration [1]. The flexural vibration of thin plates with various boundary conditions has been attracting researchers for a long time. And a large number of papers on the flexural vibration have been published, such as the highly referenced [2–12]. In these papers, various methods including numerical, analytical, and semianalytical methods have been developed to analyze the vibration characteristics of plates under various boundary conditions. Maury et al. [3] studied the response of excited panels by the wave propagation method. Gorman [4, 5] and Mochida [8] used the superposition-Galerkin method to study the vibration characteristics of rectangular plates under free boundary condition. Li [9] proposed an exact series solution for the transverse vibration of beams under general elastic boundary restraints. Besides, flexural vibration of thin plates is also studied by other researchers with FE method, DQ method DSC method [10–12], and so on.

Probably since the first nonzero natural frequency of in-plane vibration of a thin plate is much higher than the flexural vibration of the plate, compared with the transverse vibration problem, the in-plane vibration problem of plates is far less investigated in the past. As the in-plane vibration plays an important role in structural vibration, the in-plane vibration analysis has attracted attention of researchers in recent years. Many researchers have investigated the in-plane vibrations of plates with various methods [13–20]. Gorman [13, 14] analyzed the free in-plane vibration characteristics of plates with different kinds of boundary conditions by the superposition method. Farag and Pan [17, 18] studied the modal characteristics of the plate which

has two clamped parallel edges and two completely free parallel edges. It should be mentioned that Xing and Liu [19] solved all possible exact solutions about in-plane vibrations of rectangular plates.

Due to practical engineering requirements, it is often necessary to open a hole on a plate, for example, opening a hole on a steel plate to reduce the weight of the structure. So, it is necessary to study the in-plane and flexural vibration of rectangular plates with cutouts. As the transverse vibration of the plate has been studied for a long time, the transverse vibration of the rectangular plate with all kinds of cutouts also has been extensively studied. Several ways have been applied to handle the vibration problem of plates with cutouts. As illustrated in [21], the cutout on the plate is considered as an extremely thin plate. Kwaka and Han [22] used the coordinate coupling method to study the vibration of the plate with cutout under free boundary condition. Laura et al. [23] studied the out-of-plane vibration of the plate with rectangular cutout with simple supported boundary condition. And the out-of-plane vibration of plates with two rectangular cutouts is studied in Reference [24]. In this paper, plates with different kinds of rectangular cutouts are studied.

Just as illustrated previously, neither the in-plane vibrations of the plate nor the plate with different kinds of cutouts is seldom studied. Among the available papers, Shufrin and Esienberger [25] used the multiterm extended Kantorovich method to study the in-plane vibration of the plate with rectangular cutouts. In their paper, the in-plane vibration of the rectangular plate with inner or corner cutout is studied. Chen et al. [26] used the Chebyshev–Lagrangian method to study the out-of-plane and in-plane vibration of the rectangular plate with rectangular cutout.

In this paper, a modified Fourier–Ritz method is employed to analyze the vibration of the rectangular plate with cutout under arbitrary boundary conditions, aiming to provide a unified procedure for many cases, such as plate with various locations (inner corner or edge) or sizes of rectangular cutout, or different kinds of boundary conditions. The arbitrary boundary conditions can be obtained by setting the stiffness constant of the boundary springs at proper values. Under the current framework, the in-plane and flexural displacements of the rectangular plate with cutout are expanded in the form of standard Fourier series and eight auxiliary polynomials. The use of the auxiliary polynomial functions can eliminate potential discontinuities and accelerate convergence of the expanded Fourier series. The natural frequencies and mode results of plates with rectangular cutouts are obtained by using the Rayleigh–Ritz procedure.

2. Theoretical Formulations

2.1. The Model and Stress-Strain Relations of the Restrained Plate. Consider an elastically restrained plate with length L_x, width L_y, and thickness h, as depicted in Figure 1. A Descartes coordinate is fixed at the middle surface of the rectangular plate. x, y, and z represent the directions of length, width, and thickness, respectively. u, v, and w are

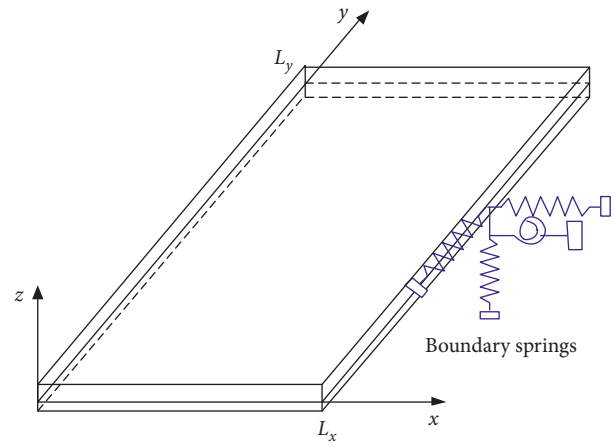

Figure 1: Rectangular plate with elastic boundary restraints.

employed to denote the displacements at the midplane of the rectangular plate in directions of x, y, and z, separately. Under the current framework, the arbitrary boundary conditions of a rectangular plate can be simulated by setting three groups of linear springs (k_u, k_v, k_w) and a group of rotational spring (k_w) which are fixed uniformly along the boundaries of the rectangular plate at proper values. And arbitrary boundary conditions can be achieved by setting the stiffness constants of the four sets of the springs at proper values. According to Kirchhoff assumptions, the displacements of a thin plate in x, y, and z directions can be written as follows:

$$\begin{aligned} U(x,y,z) &= u(x,y) - z\frac{\partial w(x,y)}{\partial x}, \\ V(x,y,z) &= v(x,y) - z\frac{\partial w(x,y)}{\partial y}, \\ W(x,y,z) &= w(x,y), \end{aligned} \tag{1}$$

where U, V, and W represent the displacements of the plate in directions of x, y, and z, respectively. Based on the thin plate theory, the relationship between the strains and displacements of thin plates can be written as follows:

$$\begin{aligned} \varepsilon_x &= \varepsilon_x^0 + z\chi_x, \\ \varepsilon_y &= \varepsilon_y^0 + z\chi_y, \\ \gamma_{xy} &= \gamma_{xy}^0 + z\chi_{xy}, \end{aligned} \tag{2}$$

where ε_x^0 and ε_y^0 are the normal strains in the midplane of the rectangular plate and γ_{xy}^0 is the shear strain in the midplane of the rectangular plate. χ_x and χ_y represent curvature changes and χ_{xy} represents twist change, separately. They can be expressed as

$$\varepsilon_x^0 = \frac{\partial u}{\partial x}, \tag{3}$$

$$\varepsilon_\beta^0 = \frac{\partial v}{\partial y}, \tag{4}$$

$$\gamma_{xy}^{0} = \frac{\partial v}{\partial x} + \frac{\partial u}{\partial y}, \tag{5}$$

$$\chi_x = -\frac{\partial^2 w}{\partial x^2}, \tag{6}$$

$$\chi_y = -\frac{\partial^2 w}{\partial y^2}, \tag{7}$$

$$\chi_{xy} = -2\frac{\partial^2 w}{\partial x \partial y}. \tag{8}$$

Equations (3)–(8) represent the relationship between the strain and displacement of a thin plate in Descartes coordinates. Based on Hook's law, the stress-strain equations are described as

$$\begin{Bmatrix} \sigma_x \\ \sigma_y \\ \sigma_z \\ \tau_{yz} \\ \tau_{xz} \\ \tau_{xy} \end{Bmatrix} = \begin{bmatrix} Q_{11} & Q_{12} & Q_{13} & Q_{14} & Q_{15} & Q_{16} \\ Q_{21} & Q_{22} & Q_{23} & Q_{24} & Q_{21} & Q_{26} \\ Q_{31} & Q_{32} & Q_{33} & Q_{34} & Q_{31} & Q_{36} \\ Q_{41} & Q_{42} & Q_{43} & Q_{44} & Q_{41} & Q_{46} \\ Q_{51} & Q_{52} & Q_{53} & Q_{54} & Q_{51} & Q_{56} \\ Q_{61} & Q_{62} & Q_{63} & Q_{64} & Q_{61} & Q_{66} \end{bmatrix} \begin{Bmatrix} \varepsilon_x \\ \varepsilon_y \\ \varepsilon_z \\ \gamma_{yz} \\ \gamma_{xz} \\ \gamma_{xy} \end{Bmatrix}, \tag{9}$$

where

$$\begin{bmatrix} Q_{11} & Q_{12} & Q_{13} & Q_{14} & Q_{15} & Q_{16} \\ Q_{21} & Q_{22} & Q_{23} & Q_{24} & Q_{21} & Q_{26} \\ Q_{31} & Q_{32} & Q_{33} & Q_{34} & Q_{31} & Q_{36} \\ Q_{41} & Q_{42} & Q_{43} & Q_{44} & Q_{41} & Q_{46} \\ Q_{51} & Q_{52} & Q_{53} & Q_{54} & Q_{51} & Q_{56} \\ Q_{61} & Q_{62} & Q_{63} & Q_{64} & Q_{61} & Q_{66} \end{bmatrix} = \begin{bmatrix} \frac{E}{1-\mu^2} & \frac{\mu E}{1-\mu^2} & \cdots & 0 \\ \frac{\mu E}{1-\mu^2} & \frac{E}{1-\mu^2} & \cdots & 0 \\ \vdots & \vdots & \ddots & \vdots \\ 0 & 0 & \cdots & \frac{E}{2(1+\mu)} \end{bmatrix}, \tag{10}$$

where σ_x, σ_y, and σ_z represent the normal stress of a rectangular plate in the direction of x, y, and z, respectively. E and μ are Young's modulus and Poisson's ratio of the plate, respectively.

Performing the integration of stresses $(\sigma_x, \sigma_y, \tau_{xy})$ over the thickness of the plate, we get

$$\begin{bmatrix} N_x & N_y & N_{xy} \end{bmatrix} = \int_{-(h/2)}^{h/2} \begin{bmatrix} \sigma_x & \sigma_y & \tau_{xy} \end{bmatrix} dz, \tag{11}$$

$$\begin{bmatrix} M_x & M_y & M_{xy} \end{bmatrix} = \int_{-(h/2)}^{h/2} \begin{bmatrix} \sigma_x & \sigma_y & \tau_{xy} \end{bmatrix} z\, dz. \tag{12}$$

Performing Equations (11) and (12) yields, we get

$$\begin{bmatrix} N_x \\ N_y \\ N_{xy} \\ M_x \\ M_y \\ M_{xy} \end{bmatrix} = \begin{bmatrix} A_{11} & A_{12} & A_{16} & B_{11} & B_{12} & B_{16} \\ A_{21} & A_{22} & A_{26} & B_{21} & B_{22} & B_{26} \\ A_{61} & A_{62} & A_{66} & B_{61} & B_{62} & B_{66} \\ B_{11} & B_{12} & B_{16} & D_{11} & D_{12} & D_{16} \\ B_{21} & B_{22} & B_{26} & D_{21} & D_{22} & D_{26} \\ B_{61} & B_{62} & B_{66} & D_{61} & D_{62} & D_{66} \end{bmatrix} \begin{bmatrix} \varepsilon_x^0 \\ \varepsilon_y^0 \\ \gamma_{xy}^0 \\ \chi_x \\ \chi_y \\ \chi_{xy} \end{bmatrix}, \tag{13}$$

where

$$\begin{bmatrix} A_{11} & A_{12} & A_{16} & B_{11} & B_{12} & B_{16} \\ A_{21} & A_{22} & A_{26} & B_{21} & B_{22} & B_{26} \\ A_{61} & A_{62} & A_{66} & B_{61} & B_{62} & B_{66} \\ B_{11} & B_{12} & B_{16} & D_{11} & D_{12} & D_{16} \\ B_{21} & B_{22} & B_{26} & D_{21} & D_{22} & D_{26} \\ B_{61} & B_{62} & B_{66} & D_{61} & D_{62} & D_{66} \end{bmatrix} = \begin{bmatrix} \frac{Eh}{1-\mu^2} & \frac{\mu Eh}{1-\mu^2} & 0 & 0 & 0 & 0 \\ \frac{\mu Eh}{1-\mu^2} & \frac{Eh}{1-\mu^2} & 0 & 0 & 0 & 0 \\ 0 & 0 & \frac{\mu Eh}{2(1+\mu)} & 0 & 0 & 0 \\ 0 & 0 & 0 & \frac{Eh^3}{12(1-\mu^2)} & \frac{\mu Eh^3}{12(1-\mu^2)} & 0 \\ 0 & 0 & 0 & \frac{\mu Eh^3}{12(1-\mu^2)} & \frac{Eh^3}{12(1-\mu^2)} & 0 \\ 0 & 0 & 0 & 0 & 0 & \frac{Eh^3}{6(1+\mu)} \end{bmatrix}, \tag{14}$$

where N_x and N_y are defined as the force resultants and N_{xy} is defined as the shear force resultant. M_x and M_y are defined as bending resultants and M_{xy} is defined as the twist moment resultant, respectively.

By now, all the stress-strain relations and other needed equations are obtained, and they will be used to derive the energy functions of the rectangular plate with small deformation.

2.2. Energy Functions. In this paper, the Rayleigh–Ritz procedure is employed to solve the vibration problems of a rectangular plate. Thus, the energy functions of the plate should be obtained first. For vibration analysis, the Lagrange energy function (L) of the rectangular plate is defined as

$$L = T - U_s - U_{sp}, \tag{15}$$

where T, U_s, and U_{sp} are kinetic energy of the rectangular plate, potential energy of the rectangular plate, and the potential energy stored in the boundary springs, respectively.

Based on the classical thin plate theory (CPT), the potential energy (U_s) of a rectangular plate in Equation (15) can be rewritten as

$$\begin{aligned} U_s = \frac{1}{2}\int_0^a \int_0^b \{&N_x\varepsilon_x^0 + N_y\varepsilon_y^0 + N_{xy}\gamma_{xy}^0 \\ &+ M_x\chi_x + M_y\chi_y + M_{xy}\chi_{xy}\}dx\,dy. \end{aligned} \tag{16}$$

Inserting Equation (13) into Equation (16), the potential energy equation of the rectangular plate can be described as

$$\begin{aligned} U_s = \frac{1}{2}\int_0^a \int_0^b K\left(\left(\varepsilon_x^0\right)^2 + 2\mu\varepsilon_x^0\varepsilon_y^0 + \left(\varepsilon_y^0\right)^2 + \frac{1-\mu}{2}\left(\gamma_{xy}^0\right)^2\right)dx\,dy \\ + \frac{1}{2}\int_0^a \int_0^b D\left(\chi_x^2 + 2\mu\chi_x\chi_y + \chi_y^2 + \frac{1-\mu}{2}\chi_{xy}^2\right)dx\,dy. \end{aligned} \tag{17}$$

And the kinetic energy (T) of the rectangular plates is written as

$$T = \frac{\rho h}{2}\int_0^a \int_0^b \left\{\left(\frac{\partial u}{\partial t}\right)^2 + \left(\frac{\partial v}{\partial t}\right)^2 + \left(\frac{\partial w}{\partial t}\right)^2\right\}dx\,dy, \tag{18}$$

where ρ and h are the density and the thickness of the rectangular plate, respectively.

As Laura et al. illustrated in [23], a rectangular plate with a hole can be regarded as a structure combined by two kinds of different materials. And the material properties of the hole on the plate can be considered as $\rho = 0$ kg/m^3, $E = 0$ GPa, and $\mu = 0$. Thus, the Lagrange energy equation of a rectangular plate with rectangular cutout can be obtained in this method. In order to describe this problem clearly, one specific example is presented here. Consider a rectangular plate with one inner cutout, as shown in Figure 2. The length and width of the plate are L_x and L_y. The location of the cutout can be described by the coordinates of the corners of the cutout, and the coordinates of the corners are $A(L_{x0}, L_{y0})$ and $B(L_{x1}, L_{y1})$. Thus, the potential energy equations of the structure depicted in Figure 2 can be written as

$$\begin{aligned} U_s = &\frac{1}{2}K\left(\int_0^{L_{y0}}\int_0^{L_x} + \int_{L_{y0}}^{L_{y1}}\int_0^{L_{x0}} + \int_{L_{y0}}^{L_{y1}}\int_{L_{x1}}^{L_x} + \int_{L_{y1}}^{L_y}\int_0^{L_x}\right)M_1 dx\,dy \\ &+ \frac{1}{2}D\left(\int_0^{L_{y0}}\int_0^{L_x} + \int_{L_{y0}}^{L_{y1}}\int_0^{L_{x0}} + \int_{L_{y0}}^{L_{y1}}\int_{L_{x1}}^{L_x} + \int_{L_{y1}}^{L_y}\int_0^{L_x}\right)M_2 dx\,dy, \end{aligned} \tag{19}$$

where

$$M_1 = \left(\varepsilon_x^0\right)^2 + 2\mu\varepsilon_x^0\varepsilon_y^0 + \left(\varepsilon_y^0\right)^2 + \frac{1-\mu}{2}\left(\gamma_{xy}^0\right)^2, \tag{20}$$

$$M_2 = \chi_x^2 + 2\mu\chi_x\chi_y + \chi_y^2 + \frac{1-\mu}{2}\chi_{xy}^2. \tag{21}$$

As illustrated previously, the general boundary conditions can be achieved by setting the stiffness constant of boundary springs at proper values. In this paper, k_ψ^u, k_ψ^v, k_ψ^w, and k_ψ^r are adopted to represent the stiffness constants of the boundary springs which are fixed along the four edges of the rectangular plate $x = 0$, $y = 0$, $x = a$, and $y = b$, respectively. Thus, the potential energy stored in the boundary springs can be written as

$$\begin{aligned} U_{sp} = &\frac{1}{2}\int_0^b \left\{\left[k_{x0}^u u^2 + k_{x0}^v v^2 + k_{x0}^w w^2 + k_{x0}^r\left(\frac{\partial w}{\partial x}\right)^2\right]\Bigg|_{x=0}\right. \\ &\left. + \left[k_{x1}^u u^2 + k_{x1}^v v^2 + k_{x1}^w w^2 + k_{x1}^r\left(\frac{\partial w}{\partial x}\right)^2\right]\Bigg|_{x=a}\right\}dy \\ &+ \frac{1}{2}\int_0^a \left\{\left[k_{y0}^u u^2 + k_{y0}^v v^2 + k_{y0}^w w^2 + k_{y0}^r\left(\frac{\partial w}{\partial y}\right)^2\right]\Bigg|_{y=0}\right. \\ &\left. + \left[k_{y1}^u u^2 + k_{y1}^v v^2 + k_{y1}^w w^2 + k_{y1}^r\left(\frac{\partial w}{\partial y}\right)^2\right]\Bigg|_{y=b}\right\}dx. \end{aligned} \tag{22}$$

According to the Rayleigh–Ritz procedure, choosing suitable displacement functions is of great importance to make the approximate solutions converge to the exact solutions.

The displacement of a rectangular plate can be theoretically expressed in any group of orthogonal polynomials. However, since computers have the round-off errors, the high-order polynomials generally become numerically instable. For the plates under arbitrary boundary conditions, the displacement functions expressed in the form of standard Fourier cosine or sine series can avoid this problem, but discontinuities of the displacement functions and their derivatives will potentially exist along the boundaries of the rectangular plates. This kind of problem is demonstrated in detail [27–33]. In order to overcome this difficulty, the modified Fourier series is employed, and the displacement of the plate is expressed as follows:

$$u(x,y) = \sum_{m=0}^{\infty}\sum_{n=0}^{\infty} A_{mn}\cos\lambda_{am}x\cos\lambda_{bn}y + P(x,y), \tag{23}$$

$$v(x,y) = \sum_{m=0}^{\infty}\sum_{n=0}^{\infty} B_{mn}\cos\lambda_{am}x\cos\lambda_{bn}y + Q(x,y), \tag{24}$$

$$w(x,y) = \sum_{m=0}^{\infty}\sum_{n=0}^{\infty} C_{mn}\cos\lambda_{am}x\cos\lambda_{bn}y + E(x,y), \tag{25}$$

$$P(x,y) = \sum_{m=0}^{\infty}\sum_{l=1}^{2} A_{ml}\cos\lambda_{am}x\xi_l(y) + \sum_{l=1}^{2}\sum_{n=0}^{\infty} A_{\ln}\xi_l(x)\cos\lambda_{bn}y, \tag{26}$$

$$Q(x,y) = \sum_{m=0}^{\infty}\sum_{l=1}^{2} B_{ml}\cos\lambda_{am}x\xi_l(y) + \sum_{l=1}^{2}\sum_{n=0}^{\infty} B_{\ln}\xi_l(x)\cos\lambda_{bn}y, \tag{27}$$

$$E(x,y) = \sum_{m=0}^{\infty}\sum_{l=1}^{4} E_{ml}\cos\lambda_{am}x\zeta_l(y) + \sum_{l=1}^{4}\sum_{n=0}^{\infty} E_{\ln}\zeta_l(x)\cos\lambda_{bn}y, \tag{28}$$

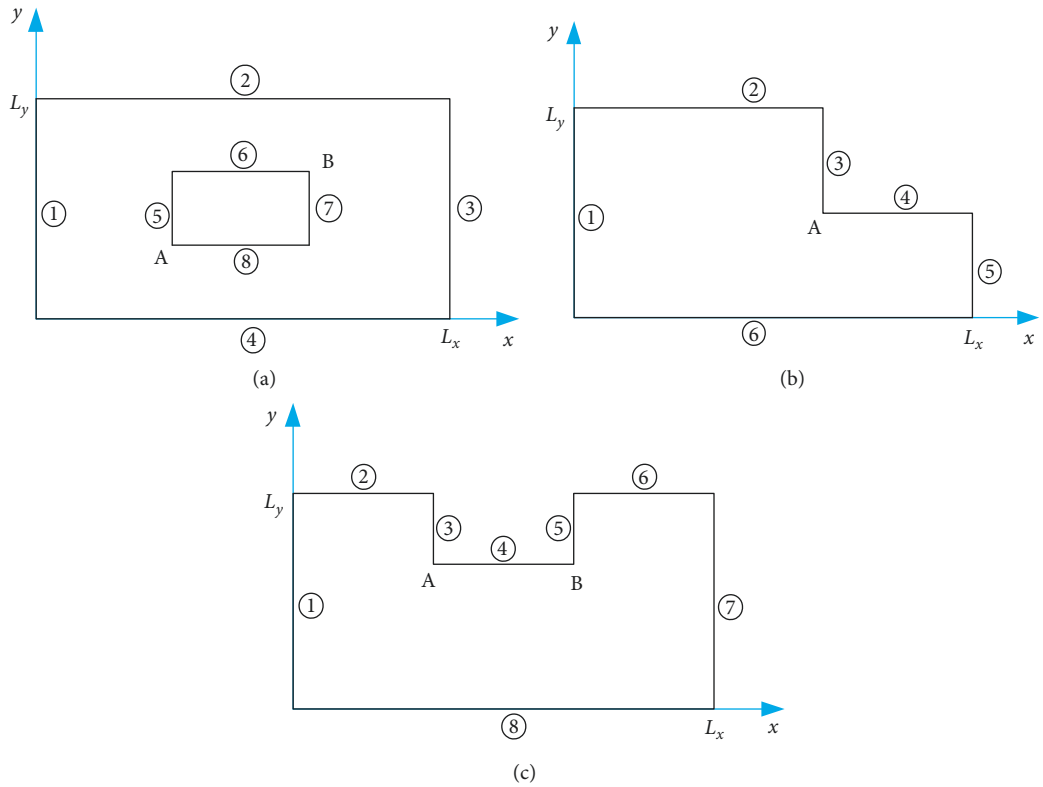

FIGURE 2: Models of plate with rectangular cutout: (a) plate with inner cutout; (b) plate with corner cutout; and (c) plate with edge cutout.

where $\lambda_{am} = m\pi/L_x, \lambda_{bn} = n\pi/L_y$, and A_{mn}, B_{mn}, C_{mn} are the coefficients of expansions in Equations (23)–(25); $A_{ml}, A_{\ln}$, $B_{ml}, B_{\ln}, C_{ml}$, and $C_{\ln}$ are the coefficients of eight auxiliary polynomials in Equations (26)–(28); and ξ_l and ζ_l are eight auxiliary polynomial functions. Displacements in the mid-plane expressed in the form of standard cosine Fourier series plus eight auxiliary polynomials can eliminate the potential discontinuity along the boundary of the plate. The eight auxiliary polynomial functions are

$$\begin{aligned}
\xi_1(\alpha) &= \alpha\left(\frac{\alpha}{L_\alpha} - 1\right)^2, \\
\xi_2(\alpha) &= \frac{\alpha^2}{L_\alpha}\left(\frac{\alpha}{L_\alpha} - 1\right), \\
\zeta_1(\alpha) &= \frac{9L_\alpha}{4\pi}\sin\left(\frac{\pi\alpha}{2L_\alpha}\right) - \frac{L_\alpha}{12\pi}\sin\left(\frac{3\pi\alpha}{2L_\alpha}\right), \\
\zeta_2(\alpha) &= -\frac{9L_\alpha}{4\pi}\cos\left(\frac{\pi\alpha}{2L_\alpha}\right) - \frac{L_\alpha}{12\pi}\cos\left(\frac{3\pi\alpha}{2L_\alpha}\right), \\
\zeta_3(\alpha) &= \frac{L_\alpha^3}{\pi^3}\sin\left(\frac{\pi\alpha}{2L_\alpha}\right) - \frac{L_\alpha^3}{3\pi^3}\sin\left(\frac{3\pi\alpha}{2L_\alpha}\right), \\
\zeta_4(\alpha) &= -\frac{L_\alpha^3}{\pi^3}\cos\left(\frac{\pi\alpha}{2L_\alpha}\right) - \frac{L_\alpha^3}{3\pi^3}\cos\left(\frac{3\pi\alpha}{2L_\alpha}\right).
\end{aligned} \tag{29}$$

Specifically, symbols α and L_α ($\alpha = x, y$, $L_\alpha = L_x, L_y$) represent independent variables and length, respectively. And it is obvious that

$$\begin{aligned}
&\zeta_1'(0) = \zeta_3'''(0) = \zeta_2'(L) = \zeta_4'''(L) = 1, \\
&\xi_1(0) = \xi_1(L) = \xi_1'(L) = 0, \\
&\xi_1'(0) = 1, \\
&\xi_2(0) = \xi_2(L) = \xi_2'(0) = 0, \\
&\xi_2'(L) = 1.
\end{aligned} \tag{30}$$

As the Lagrange energy function and the displacement functions of the rectangular plate are established, the next task is to obtain the value of the coefficients in the displacement functions. Substituting Equations (16)–(20) into the Lagrange energy function and minimizing the Lagrange energy functions by making the derivatives of the unknown variables of expansions equal to zero as

$$\begin{aligned}
&\frac{\partial L}{\partial E} = 0, \\
&E = A_{mn}, A_{ml}, A_{\ln}, B_{mn}, B_{ml}, B_{\ln}, C_{mn}, C_{ml}, C_{\ln}.
\end{aligned} \tag{31}$$

Finally, totaled $3*(M+1)*(N+1) + 12*(M+1) + 12*(N+1)$ equations are obtained and can be written in the form of matrix as

$$\left(\mathbf{K} - \omega^2\mathbf{M}\right)\mathbf{D} = 0, \tag{32}$$

where $\mathbf{K}, \mathbf{M}$, and $\mathbf{D}$ are stiffness matrix, mass matrix, and coefficient matrix, respectively. They are described as

$$\mathbf{K} = \begin{bmatrix} K_{1,1} & K_{1,2} & K_{1,3} & \cdots & K_{1,9} \\ K_{2,1} & K_{2,2} & K_{2,3} & \cdots & K_{2,9} \\ K_{3,1} & K_{3,2} & K_{3,3} & \cdots & K_{3,9} \\ \vdots & \vdots & \vdots & \ddots & \vdots \\ K_{9,1} & K_{9,2} & K_{9,3} & \cdots & K_{9,9} \end{bmatrix}, \tag{33}$$

$$\mathbf{M} = \begin{bmatrix} M_{1,1} & M_{1,2} & M_{1,3} & \cdots & M_{1,9} \\ M_{2,1} & M_{2,2} & M_{2,3} & \cdots & M_{2,9} \\ M_{3,1} & M_{3,2} & M_{3,3} & \cdots & M_{3,9} \\ \vdots & \vdots & \vdots & \ddots & \vdots \\ M_{9,1} & M_{9,2} & M_{9,3} & \cdots & M_{9,9} \end{bmatrix}, \tag{34}$$

$$\mathbf{D} = \left[D^u, D^v, D^w\right]. \tag{35}$$

The element in stiffness and mass matrix is given in Appendix. The vector **D** can be written as follows:

$$\begin{aligned} D^u &= \left[A_{00}, \ldots, A_{mn}, A_{01}, \ldots, A_{ml}, \ldots, A_{10}, \ldots, A_{\ln}\right], \\ D^v &= \left[B_{00}, \ldots, B_{mn}, B_{01}, \ldots, B_{ml}, \ldots, B_{10}, \ldots, B_{\ln}\right], \\ D^w &= \left[C_{00}, \ldots, C_{mn}, C_{01}, \ldots, C_{ml}, \ldots, C_{10}, \ldots, C_{\ln}\right]. \end{aligned} \tag{36}$$

Based on the classical thin plate theory (CPT), the in-plane and out-of-plane vibrations are decoupled, and thus the out-of-plane and in-plane vibration of a plate structure can be studied separately. When studying the flexural vibrations of the plate structure, the stiffness mass and coefficients matrix of the structure can be defined as

$$\begin{aligned} \mathbf{K}_f &= \begin{bmatrix} K_{7,7} & K_{7,8} & K_{7,9} \\ K_{8,7} & K_{8,8} & K_{8,9} \\ K_{9,7} & K_{9,8} & K_{9,9} \end{bmatrix}, \\ \mathbf{M}_f &= \begin{bmatrix} M_{7,7} & M_{7,8} & M_{7,9} \\ M_{8,7} & M_{8,8} & M_{8,9} \\ M_{9,7} & M_{9,8} & M_{9,9} \end{bmatrix}, \\ \mathbf{D}_f &= D^w. \end{aligned} \tag{37}$$

When studying the in-plane vibrations of a rectangular plate, the stiffness mass and coefficients matrix can be written as

$$\begin{aligned} \mathbf{K}_{\text{in}} &= \begin{bmatrix} K_{1,1} & K_{1,2} & K_{1,3} & \cdots & K_{1,6} \\ K_{2,1} & K_{2,2} & K_{2,3} & \cdots & K_{2,6} \\ K_{3,1} & K_{3,2} & K_{3,3} & \cdots & K_{3,6} \\ \vdots & \vdots & \vdots & \ddots & \vdots \\ K_{6,1} & K_{6,2} & K_{6,3} & \cdots & K_{6,6} \end{bmatrix}, \\ \mathbf{M}_{in} &= \begin{bmatrix} M_{1,1} & M_{1,2} & M_{1,3} & \cdots & M_{1,6} \\ M_{2,1} & M_{2,2} & M_{2,3} & \cdots & M_{2,6} \\ M_{3,1} & M_{3,2} & M_{3,3} & \cdots & M_{3,6} \\ \vdots & \vdots & \vdots & \ddots & \vdots \\ M_{6,1} & M_{6,2} & M_{6,3} & \cdots & M_{6,6} \end{bmatrix}, \\ \mathbf{D}_{\text{in}} &= \left[D^u, D^v\right]. \end{aligned} \tag{38}$$

3. Validation and Discussion

With the formulations derived in Section 2, several numerical results together with those available in the literature will be presented in this section to validate the accuracy and convergence of the current method. Besides, the vibration characteristics of the structure will also be studied.

3.1. Flexural Vibration Analysis of Rectangular Plate with Rectangular Cutouts. First, the flexural vibration of rectangular plate with one inner, edge, or corner cutout will be studied. These three kinds of models are depicted in Figure 2. The length and width of the considered rectangular plate are $L_x = L_y = 2$ m, and the thickness of the plate is $h = 0.003$ m. And the material parameters of the plate structure are defined as $E = 216$ GPa, $\mu = 0.3$, and $\rho = 7900$ kg/m^3. The coordinate of the points shown in Figure 2 are (a) $A_1\,(0.5\text{ m}, 0.5\text{ m})$ $B_1\,(1.5\text{ m}, 1.5\text{ m})$, (b) $A_2\,(1\text{ m}, 1\text{ m})$, and (c) $A_3\,(0.5\text{ m}, 1\text{ m})$ $B_3\,(1.5\text{ m}, 1\text{ m})$. For simplicity, a string consisting of several letters is adopted to represent the boundary conditions of the structure depicted in Figure 2. For example, "CCCC-FFFF" denotes the boundary conditions of the edges corresponding to number one to eight, and "C" and "F" represent clamped and free boundary conditions, respectively.

The first six nonzero natural frequencies of flexural vibration of plate structures with one cutout are listed in Table 1. The results obtained by software ANSYS are also presented here to verify the correctness of the present method. Comparing the results listed in Table 1, it can be observed that these two sets of results are very close. Besides, it can be also found that the position of the cutouts has an effect on the vibration characteristics of the structure. For example, frequency parameters in Table 1 show that the plate with one corner cutout has the largest nonzero first frequency while the plate with one edge cutout has the smallest nonzero first frequency; structures considered here are under completely free boundary conditions, and all the cutouts are also kept the same size.

By solving Equation (32), the natural frequencies and eigenvectors (**D**) can be obtained simultaneously. By inserting the eigenvector into the displacement expressions (Equations (23)–(25)), the mode shapes of the plate with one inner cutout can be acquired. The mode shapes of CCCC-FFFF plate with one inner cutout are compared with those obtained by ANSYS in Figure 3 (the right one). It can be seen that the mode shapes obtained by the present method match with those acquired by software ANSYS very well. Besides, it can also be found that with the increase of the frequency, the mode shapes of the structure become more and more complex.

The nonzero frequency parameters of the rectangular plate with one rectangular cutout in Table 1 are calculated by selecting the truncate number as $M = N = 14$. In order to check the convergence of the current method, the natural frequencies of the plate with two inner cutouts are calculated with different truncation numbers (i.e., $M_f = N_f = 7 - 13$). The models of the rectangular plate with two cutouts are depicted in Figure 4. In the following discussion, the

Table 1: Frequency parameters for flexural vibration of elastic-restrained plate with one rectangular cutout.

Mode order			1	2	3	4	5	6
Plate with inner cutout	FFFF-FFFF	Present	2.013	2.875	4.211	5.966	5.966	9.438
		ANSYS	2.008	2.870	4.204	5.949	5.949	9.298
	CCCC-FFFF	Present	12.510	14.680	14.750	20.080	20.600	27.870
		ANSYS	12.347	14.442	14.442	19.530	20.172	27.466
Plate with corner cutout	FFF-FFF	Present	2.976	3.254	5.145	6.395	11.399	11.468
		ANSYS	2.976	3.230	5.150	6.376	11.398	11.493
	CCF-FCC	Present	6.327	12.616	15.225	22.902	23.115	26.817
		ANSYS	6.325	12.529	15.210	22.811	22.997	26.769
Plate with edge cutout	FFFF-FFFF	Present	1.461	3.541	3.653	5.349	7.552	7.937
		ANSYS	1.445	3.537	3.626	5.345	7.436	7.921
	CCF-FCCC	Present	7.036	13.522	17.631	20.311	22.268	26.834
		ANSYS	6.959	13.479	17.551	20.116	21.801	26.732

geometric parameters of the plate with two cutouts are considered as 2 m in length, 2 m in width, and 0.003 m in thickness, and the material properties of the plate are defined the same as previous. The coordinates of the points shown in Figure 4 are (a) $A(0.4\text{ m}, 0.75\text{ m})$ $B(0.9\text{ m}, 1.25\text{ m})$ $C(1.1\text{ m}, 0.75\text{ m})$ $D(1.6\text{ m}, 1.25\text{ m})$, (b) $A(0.75\text{ m}, 1.5\text{ m})$ $B(1.25\text{ m}, 1.5\text{ m})$ $C(0.75\text{ m}, 0.5\text{ m})$ $D(1.25\text{ m}, 0.5\text{ m})$, and (c) $A(0.5\text{ m}, 1.5\text{ m})$ $B(1.5\text{ m}, 1.5\text{ m})$. The frequency results of the plate with two inner cutouts are listed in Table 2. It shows that the natural frequency converges at $M = N = 13$, and the convergence and numerical stability of the current method are validated.

As mentioned previously, the current method can be used to study the vibration characteristics of the rectangular plate with rectangular cutout under general elastic-restrained boundary. And the general elastic restrained boundary can be obtained by setting the stiffness constants of the boundary springs at proper values. For example, the clamped boundary conditions can be achieved by setting the stiffness constants of the linear and rotational springs as infinite. In practical calculations, a sufficiently large number is always employed to represent the "infinite." In the first example, the clamped boundary conditions are obtained by setting the stiffness constant at 10^{12}. So, effects of the stiffness constant of boundary springs on the solution results ought to be studied. The frequency parameters for EEEE-FFFF-FFFF plate with two inner rectangular cutouts are listed in Table 3, and the alphabet "E" represents elastic boundary condition. It can be found that as the stiffness constants of the springs increase, the natural frequencies of the structure increase gradually, and when the stiffness constant is beyond 10^{12}, the natural frequency remain unchanged. Thus, in the following discussion, 10^{12} is selected to represent the value of "infinite."

The mode shapes of the structure that rectangular cutouts locate inside of the plate or on the boundary of the plate or on the corner of the plate are shown in Figures 5–7, and the geometric and material parameters of the plate are kept the same as mentioned previously. Figures 5–7 show that structures shown in Figure 4 has similar mode shapes in low frequency. Besides, the mode shapes of these structures have symmetric characteristics.

As illustrated previously, the current method is able to handle the cases with arbitrary boundary conditions. The first six nonzero frequency parameters of the structure with one rectangular cutout under four kinds of boundary conditions are listed in Table 4. The rectangular plate considered is in the length of 2 m, width of 1 m, and thickness of 0.003 m, and the corner points of the cutout are located at A (0.8 m, 0.4 m) and B (1.2 m, 0.6 m). The material properties of the structure are $E = 216$ GPa, $\mu = 0.3$, and $\rho = 7900\text{ kg/m}^3$. It should be mentioned that the alphabet "S" and "C" are used to represent the simply supported and clamped boundary conditions, respectively. From Table 4, it can be found that the present results are very close to the results obtained by software ANSYS.

3.2. In-Plane Vibration Analysis of Rectangular Plate with Cutouts. The flexural vibration of the rectangular plate with cutouts has been studied in the previous section. It proves that the current method is capable of investigating the flexural vibration characteristics of the plate with rectangular cutout. Next, the in-plane vibration of the structure will be investigated. The natural frequencies and mode shapes for in-plane vibration of rectangular plate with cutouts will be presented in this section.

In order to verify the correctness of the present method, plate with one cutout is studied firstly. The first example is a classical case: plate with one cutout under the clamped boundary condition. The clamped boundary conditions can be obtained by setting the stiffness constants of the springs at 10^{12}. For this example, the geometric parameters of the rectangular plate considered here are $L_x = L_y = 3$ m and $h = 0.0025$ m, the material properties of the plate are defined as $E = 70$ GPa, $\mu = 0.33$, and $\rho = 2700\text{ kg/m}^3$, and the truncated numbers are selected as $\mathbf{M}_{\text{in}} = \mathbf{N}_{\text{in}} = 24$. The coordinates of the opposite corners of the cutouts shown in Figure 2 are (a) $A_1(0.25\text{ m}, 0.25\text{ m})$ $B_1(0.75\text{ m}, 0.75\text{ m})$, (b) $A_2(2.5\text{ m}, 2.5\text{ m})$, (c) $A_3(1.25\text{ m}, 2.5\text{ m})$ $B_3(1.75\text{ m}, 2.5\text{ m})$. The first six frequency parameters for in-plane vibration of structures with one cutout are presented in Table 5. And the mode shapes of the CCCC-FFFF plate with one inner cutout are also presented here. From Table 5 and Figure 8, it can be seen that the present results show an excellent agreement with results acquired by software ANSYS.

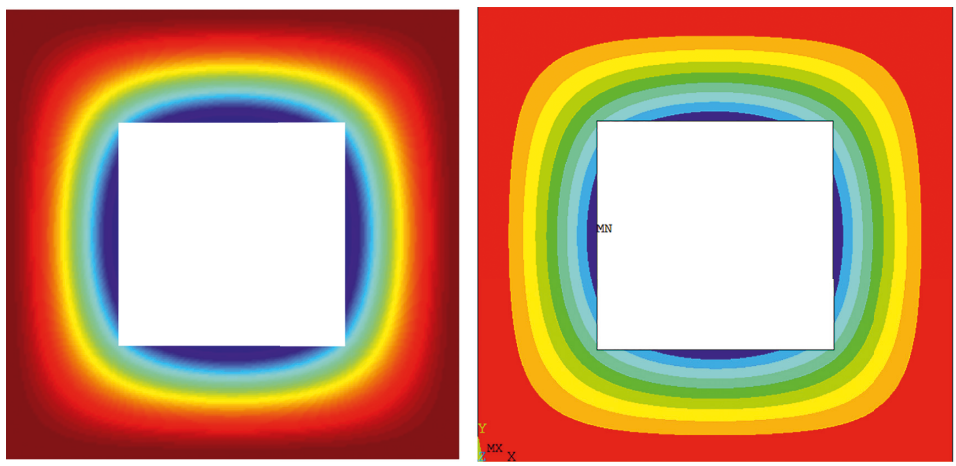

(a)

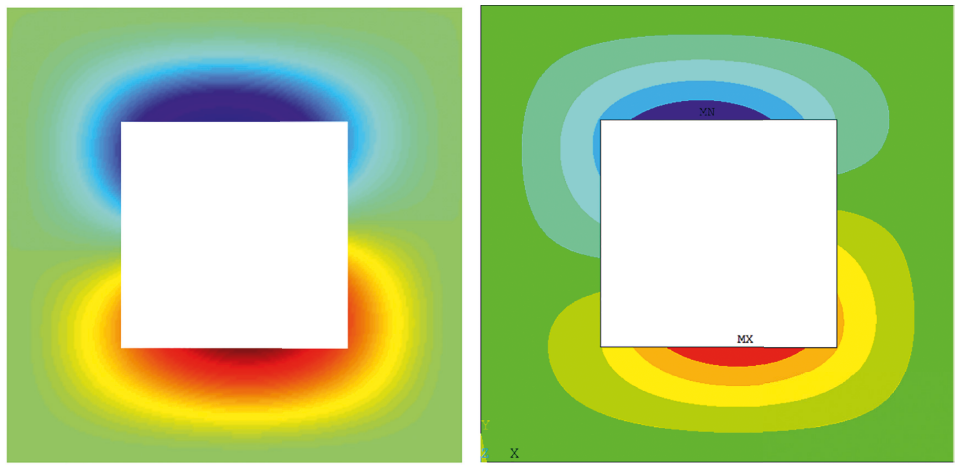

(b)

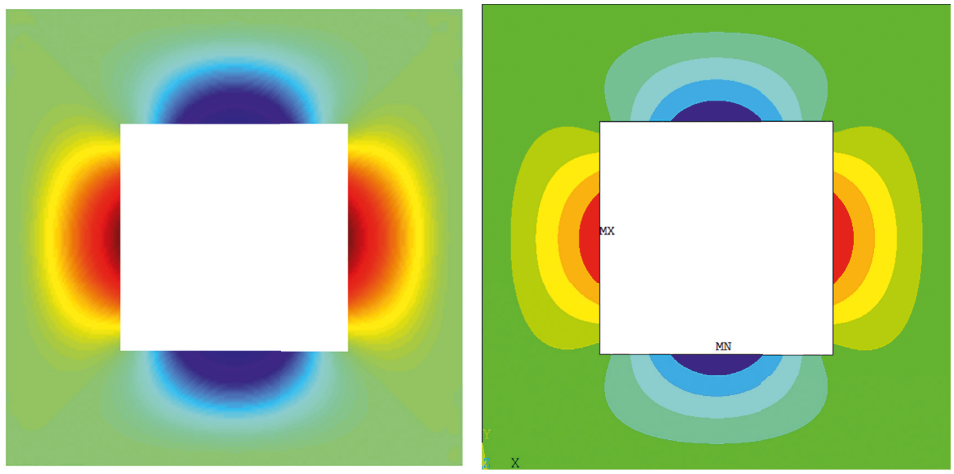

(c)

Figure 3: Continued.

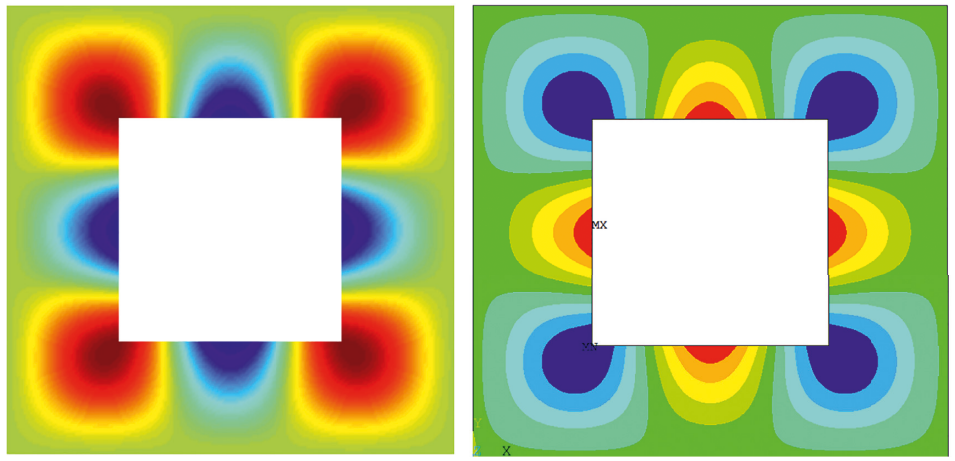

(d)

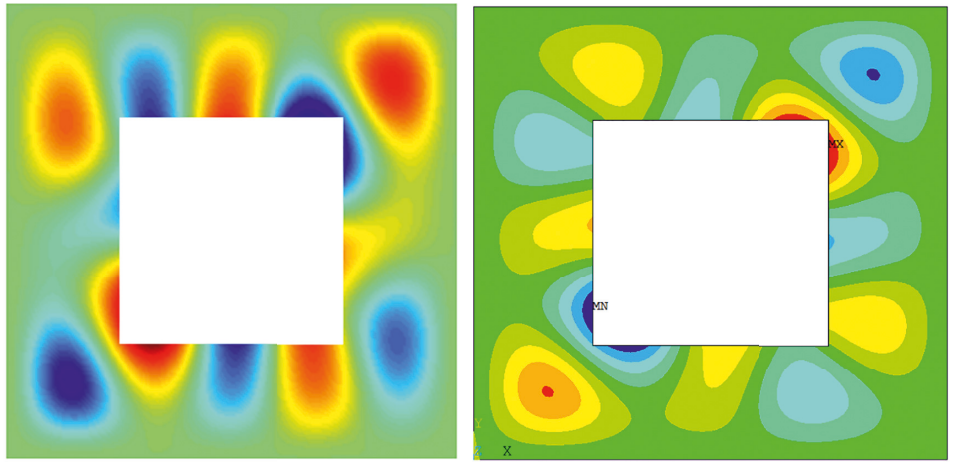

(e)

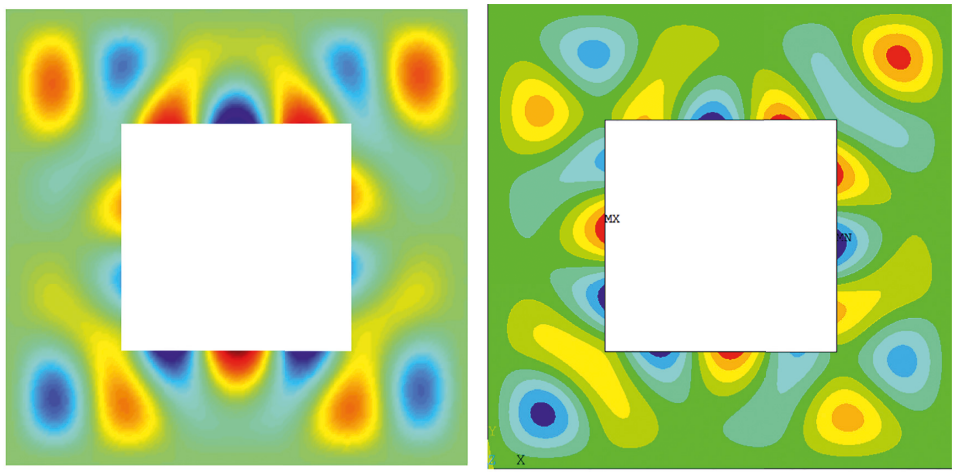

(f)

Figure 3: Continued.

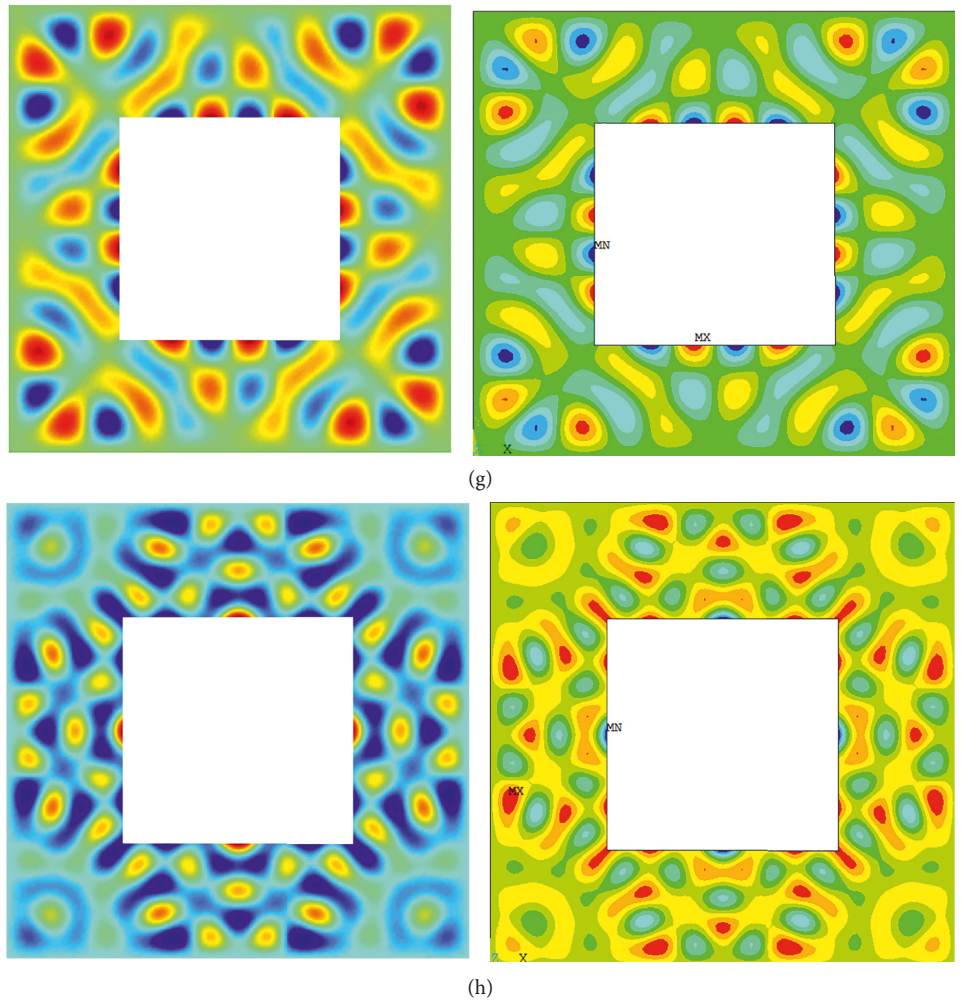

Figure 3: Mode shapes for flexural vibration of the CCCC-FFFF plate structure with one rectangular cutout locating inside of the plate: the (a) first mode shape; (b) second mode shape; (c) fourth mode shape; (d) eighth mode shape; (e) sixteenth mode shape; (f) thirty-second mode shape; (g) hundredth mode shape; and (h) two-hundredth mode shape.

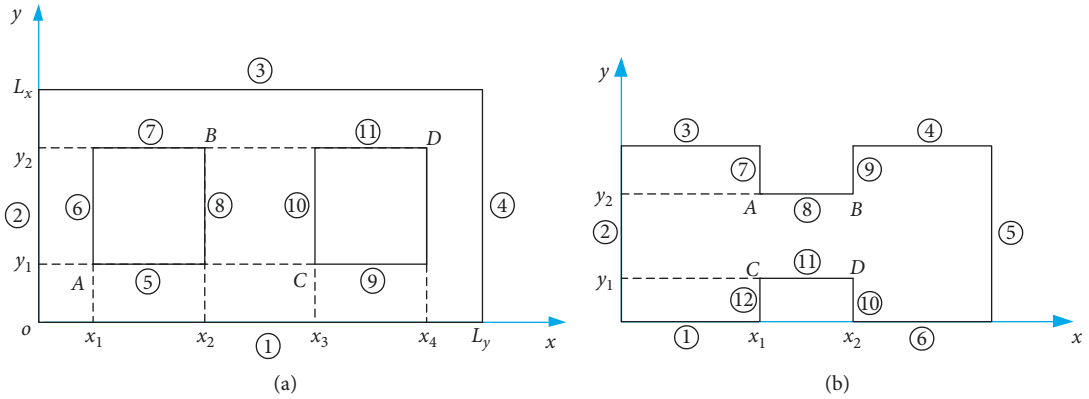

Figure 4: Continued.

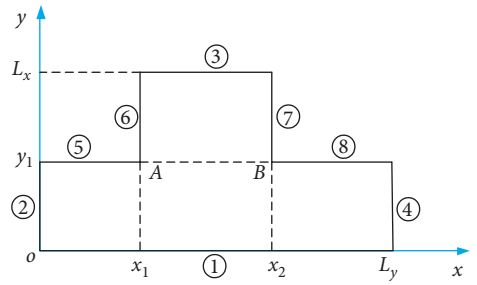

(c)

Figure 4: Models of rectangular plate with two cutouts: (a) rectangular plate with two inner cutouts; (b) rectangular plate two with edge cutouts; and (c) rectangular plate with two corner cutouts.

Table 2: Natural frequencies of FFFF-FFFF-FFFF rectangular plate with two inner cutouts in different truncation schemes.

$M = N$	1	2	3	4	5	6	7	8
7	2.30	3.26	4.07	6.22	6.45	11.04	11.13	12.12
8	2.30	3.25	4.01	6.21	6.43	11.01	11.13	11.96
9	2.29	3.25	4.01	6.20	6.43	10.84	10.98	11.96
10	2.29	3.24	4.00	6.20	6.43	10.84	10.97	11.90
11	2.29	3.24	4.00	6.19	6.42	10.60	10.95	11.90
12	2.29	3.24	3.98	6.18	6.42	10.59	10.95	11.89
13	2.29	3.24	3.98	6.18	6.41	10.45	10.93	11.89
14	2.29	3.23	3.97	6.18	6.41	10.45	10.93	11.84
15	2.29	3.23	3.97	6.17	6.41	10.38	10.92	11.84
16	2.29	3.22	3.96	6.17	6.41	10.38	10.92	11.83
17	2.29	3.22	3.96	6.17	6.41	10.38	10.92	11.83
18	2.29	3.22	3.96	6.17	6.41	10.38	10.92	11.83

Table 3: Frequency parameters of an EEEE-FFFF-FFFF plate with two inner rectangular cutouts ($K^u = K^v = K^w = K^r = k$).

	Mode order							
k	1	2	3	4	5	6	7	8
10^5	6.66	10.33	11.92	14.35	16.40	17.67	19.55	20.50
10^6	7.35	12.08	14.84	18.17	21.53	25.67	27.32	30.82
10^7	7.44	12.30	15.23	18.76	22.19	26.92	28.67	32.81
10^8	7.44	12.32	15.27	18.82	22.26	27.04	28.81	33.02
10^9	7.44	12.33	15.28	18.83	22.26	27.06	28.83	33.04
10^{10}	7.44	12.33	15.28	18.83	22.26	27.06	28.83	33.04
10^{11}	7.45	12.33	15.28	18.83	22.26	27.06	28.83	33.04
10^{12}	7.45	12.33	15.28	18.83	22.26	27.06	28.83	33.04
10^{12}	7.45	12.33	15.28	18.83	22.26	27.06	28.83	33.04
10^{14}	7.45	12.33	15.28	18.83	22.26	27.06	28.83	33.04

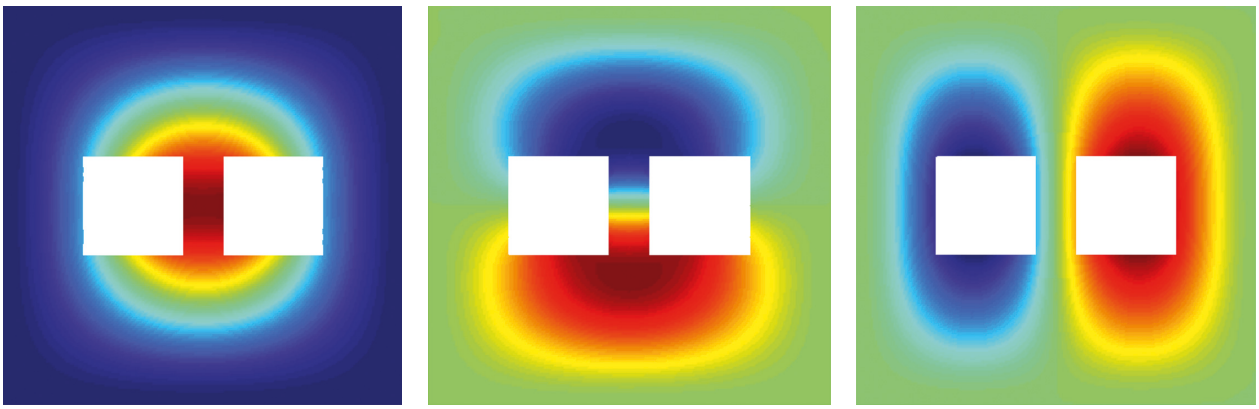

(a) (b) (c)

Figure 5: Continued.

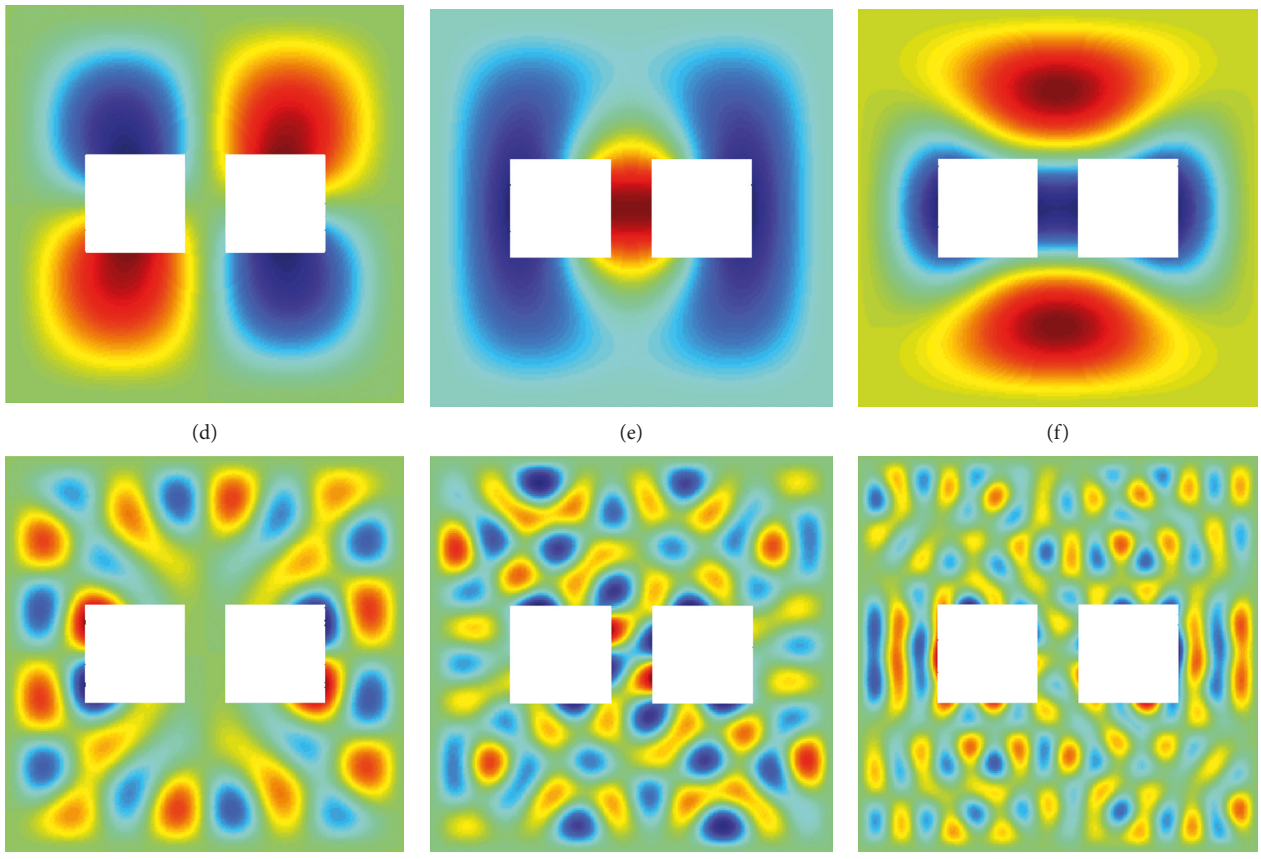

Figure 5: Mode shapes for flexural vibration of the CCCC-FFFF-FFFF plate structure with two rectangular cutouts locating inside of the plate: the (a) first mode shape; (b) second mode shape; (c) third mode shape; (d) fourth mode shape; (e) fifth mode shape; (f) sixth mode shape; (g) fiftieth mode shape; (h) hundredth mode shape; and (i) two-hundredth mode shape.

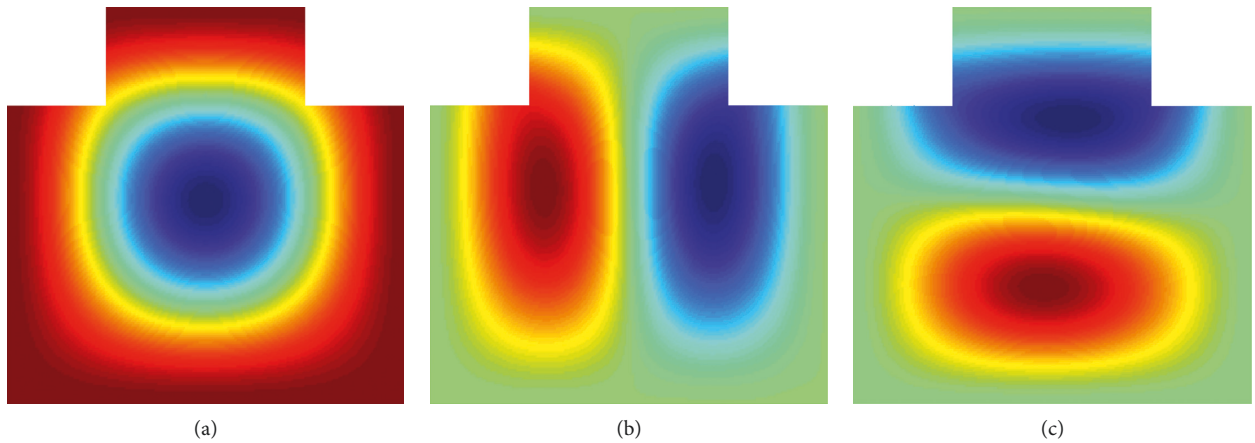

Figure 6: Continued.

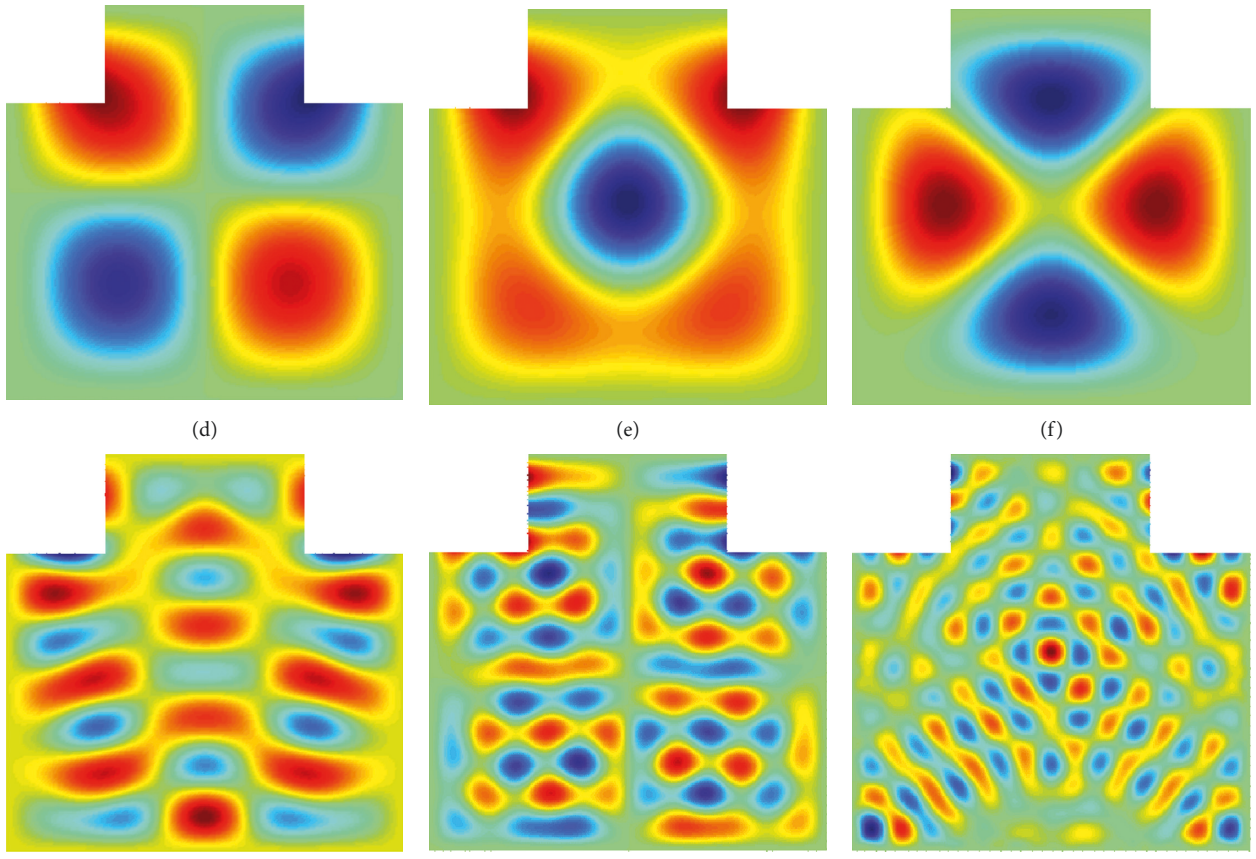

Figure 6: Mode shapes for flexural vibration of the CCCC-FFFF plate structure with two rectangular cutouts locating on corner of the plate: the (a) first mode shape; (b) second mode shape; (c) third mode shape; (d) fourth mode shape; (e) fifth mode shape; (f) sixth mode shape; (g) fiftieth mode shape; (h) hundredth mode shape; and (i) two-hundredth mode shape.

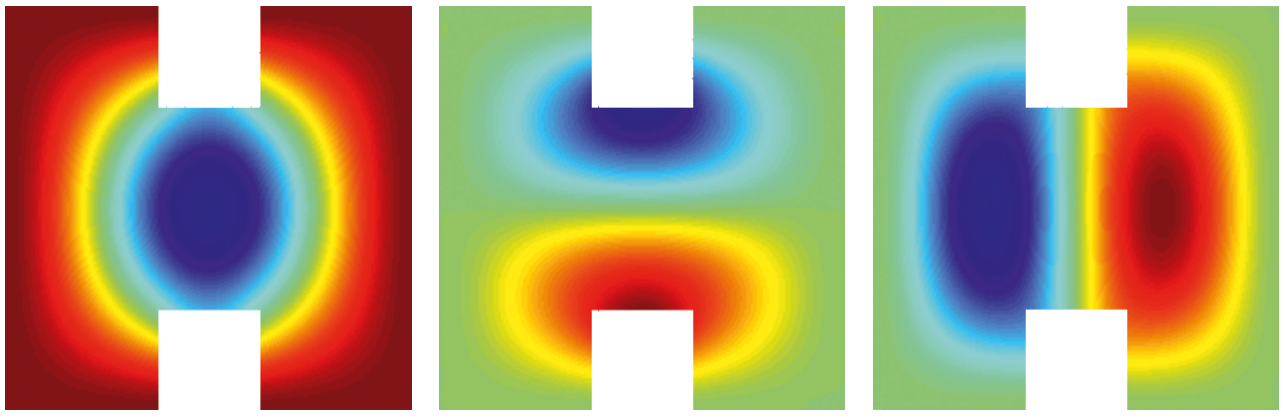

Figure 7: Continued.

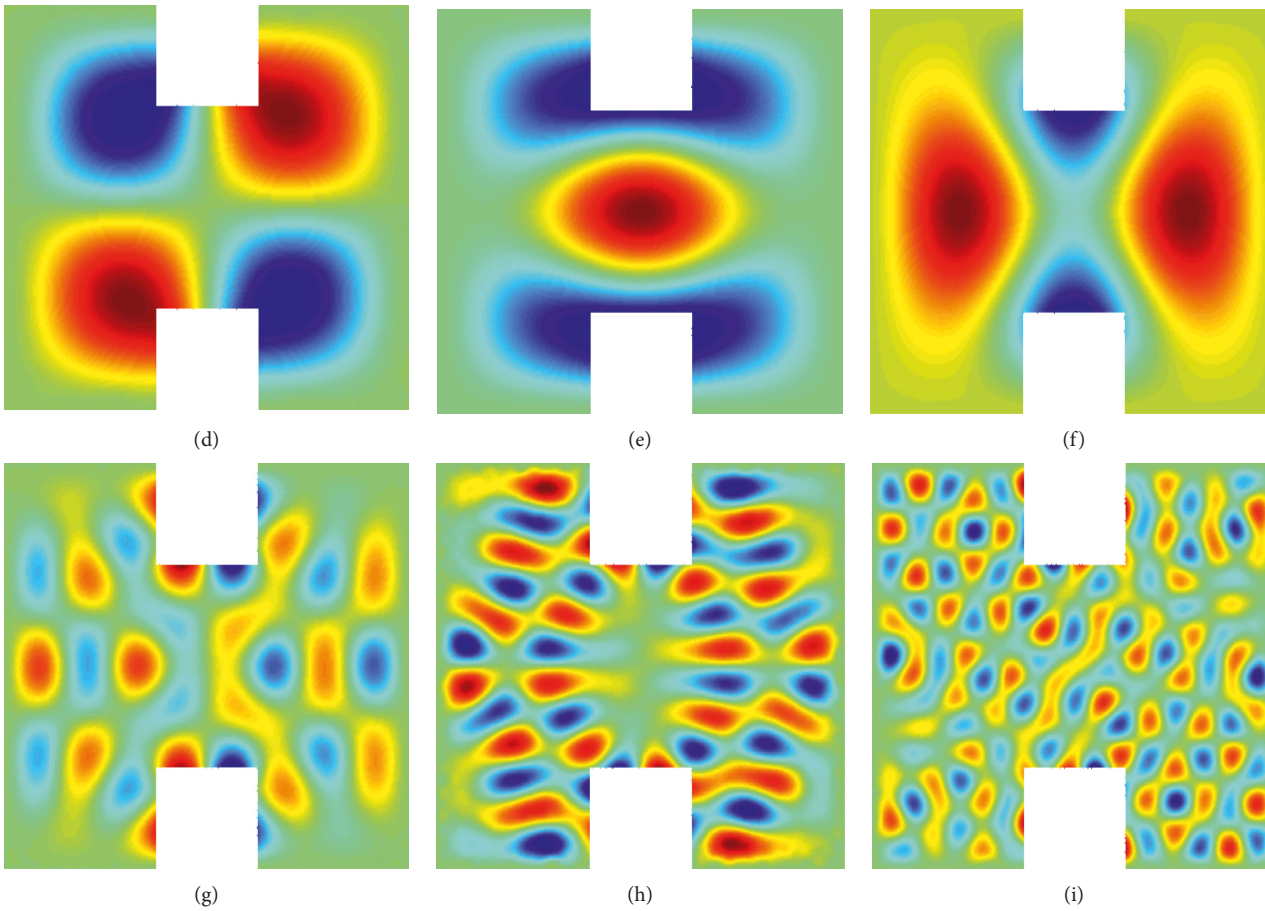

Figure 7: Mode shapes for flexural vibration of the CCCCCC-FFFFFF plate structure with two rectangular cutouts locating on boundary of the plate: the (a) first mode shape; (b) second mode shape; (c) third mode shape; (d) fourth mode shape; (e) fifth mode shape; (f) sixth mode shape; (g) fiftieth mode shape; (h) hundredth mode shape; and (i) two-hundredth mode shape.

Table 4: Frequency parameters of the structure with one cutout located inside of the plate under different kinds of boundary conditions.

Mode order		1	2	3	4	5	6	7	8
FFFF-FFFF	Present	3.904	4.815	10.977	11.171	15.429	18.809	19.560	22.139
	ANSYS	3.880	4.808	10.927	11.110	15.330	18.783	19.529	22.140
CFFF-FFFF	Present	0.634	2.710	4.004	8.997	11.299	16.489	17.105	21.917
	ANSYS	0.645	2.706	3.984	8.962	11.230	16.383	17.068	21.887
CCFF-FFFF	Present	3.183	6.898	13.680	16.725	21.370	24.889	29.914	39.087
	ANSYS	3.166	6.856	13.620	16.640	21.290	24.748	29.760	38.754
CSFF-FFFF	Present	1.572	5.839	11.533	13.173	17.061	24.273	26.066	36.552
	ANSYS	1.580	5.816	11.470	13.100	16.930	24.188	25.939	34.347

Table 5: Frequency parameters of rectangular plate with one cutout.

Mode order		1	2	3	4	5	6	7	8
Plate with inner cutout	CCCC-FFFF	964.7[a]	1004.1[a]	1157.5[a]	1436.8[a]	1618.7[a]	1640.3[a]	1658.5[a]	1906.3[a]
		959.27[b]	1003.8[b]	1155.9[b]	1432.0[b]	1615.5[b]	1637.1[b]	1658.1[b]	1902.0[b]
Plate with corner cutout	CCF-FCC	978.0[a]	1008.9[a]	1177.5[a]	1426.6[a]	1623.8[a]	1650.5[a]	1657.2[a]	1859.1[a]
		977.8[b]	1008.9[b]	1177.3[b]	1426.3[b]	1623.2[b]	1650.4[b]	1657.3[b]	1858.8[b]
Plate with edge cutout	CCFF-FCCC	946.0[a]	993.4[a]	1143.6[a]	1468.1[a]	1592.9[a]	1614.2[a]	1624.3[a]	1892.1[a]
		942.4[b]	991.2[b]	1141.0[b]	1467.7[b]	1589.6[b]	1613.5[b]	1622.9[b]	1891.3[b]

[a]present results; [b]ANSYS results.

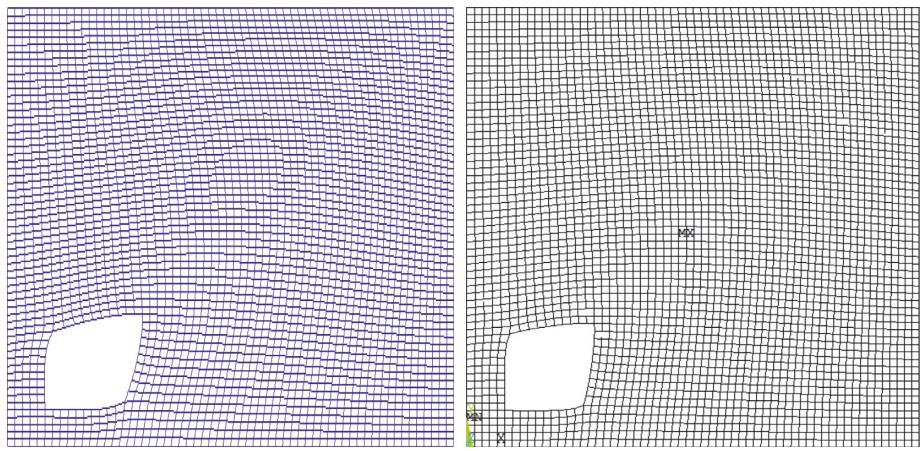

(a)

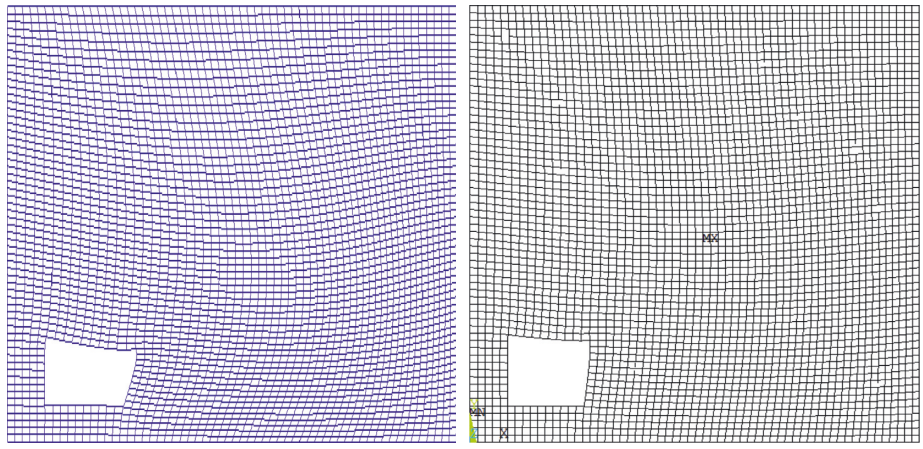

(b)

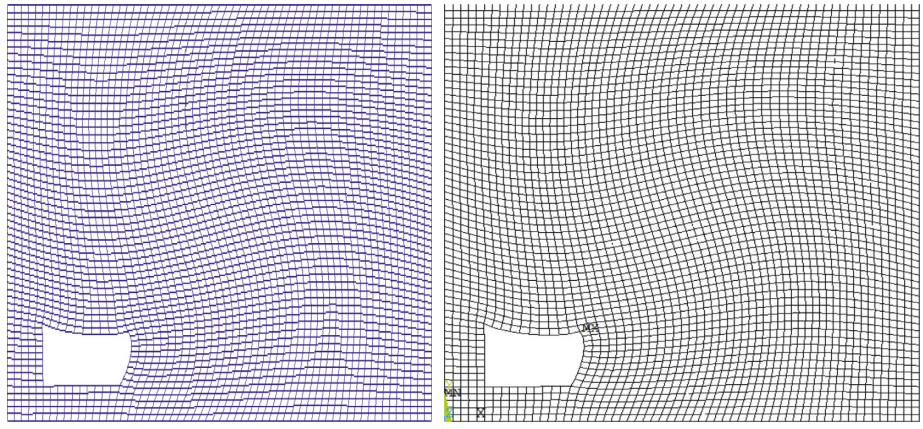

(c)

Figure 8: Continued.

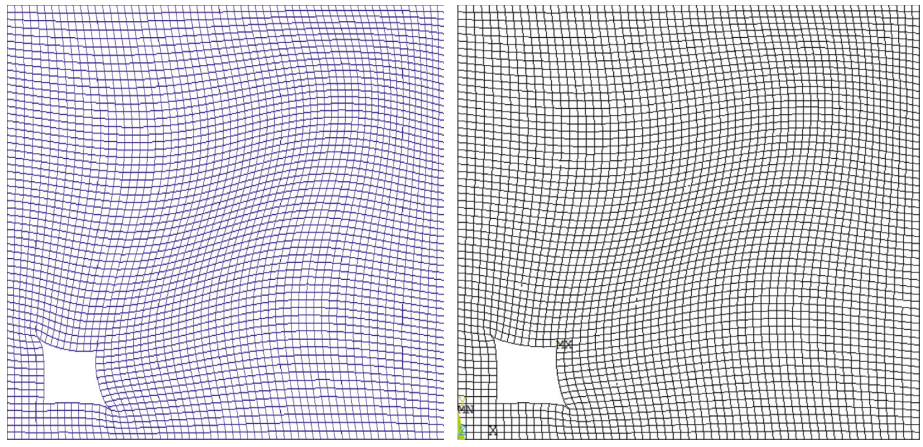

(d)

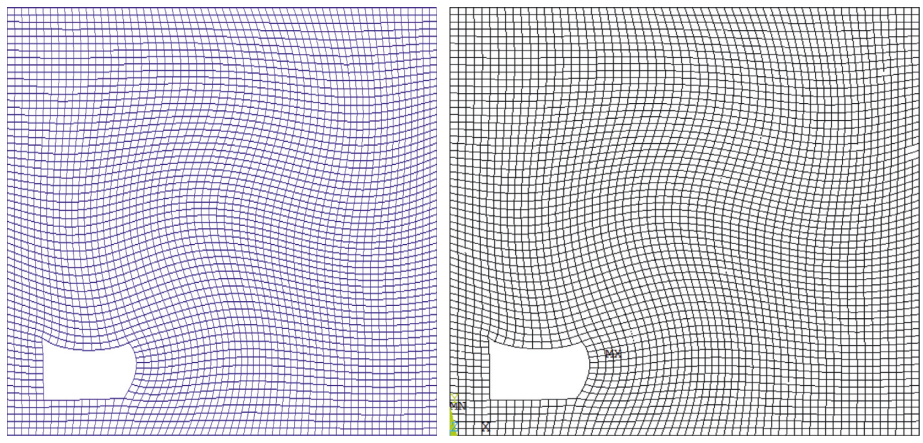

(e)

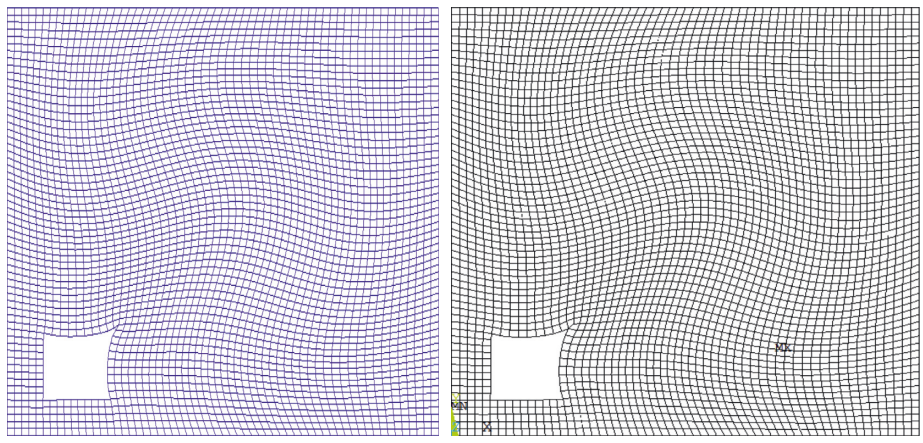

(f)

Figure 8: Continued.

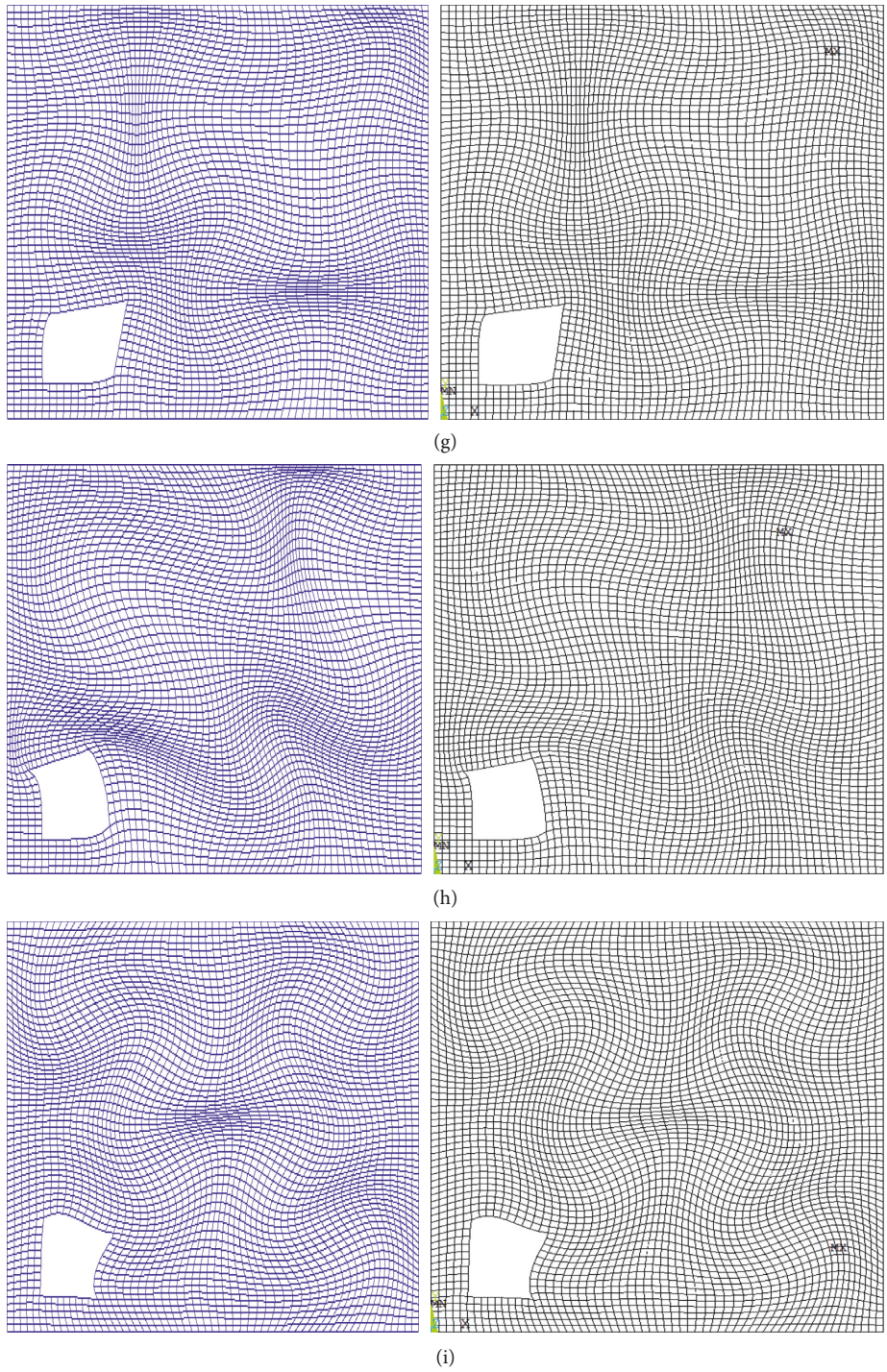

FIGURE 8: Mode shapes for in-plane vibration of the CCCC-FFFF plate structure with one rectangular cutout locating inside of the plate: the (a) first mode shape; (b) second mode shape; (c) third mode shape; (d) fourth mode shape; (e) fifth mode shape; (f) sixth mode shape; (g) twentieth mode shape; (h) twenty-first mode shape; and (i) twenty-second mode shape.

The effects of the boundary conditions on the vibration of the plate with rectangular cutout are considered here. According to [17], there exist two types of simply supported boundary conditions for in-plane vibration. The first type can be considered as stiffness constants of the tangential springs and normal springs are infinite and zero, respectively, while the second one can be seen as stiffness constants of the tangential and normal springs are zero and infinite, separately. For simplicity, these two kinds of boundary conditions are denoted by "S_t"and "S_n," respectively. The geometric and material parameters of the plate are same as the ones defined in Table 5. Table 6 shows the natural frequencies of the plate with rectangular cutout located inside of the plate under different kinds of boundary

Table 6: Frequency parameters of the plate with one inner cutout.

Mode order		1	2	3	4	5	6
CFCF-FFFF	Present	451.80	806.28	851.34	937.11	1031.56	1059.58
	ANSYS	448.66	803.85	847.42	934.39	1029.41	1055.32
CCCF-FFFF	Present	613.80	830.60	914.19	1188.37	1308.05	1349.43
	ANSYS	609.35	827.98	907.89	1182.01	1299.73	1347.12
CS_nS_tF-FFFF	Present	401.86	513.41	705.11	930.53	1065.76	1153.31
	ANSYS	400.68	509.44	704.71	921.95	1065.40	1153.22
$S_nS_nS_nS_n$-FFFF	Present	697.20	836.04	884.95	1130.19	1155.51	1222.97
	ANSYS	696.86	830.35	884.93	1125.6	1155.8	1219.3
$S_tS_tS_tS_t$-FFFF	Present	449.99	523.70	733.39	1009.46	1046.24	1111.86
	ANSYS	441.34	523.73	733.36	1004.20	1046.51	1107.60

Table 7: Frequency parameters of the FFFFFF-FFF-FFF plate with two edge rectangular cutouts.

$M = N$	1	2	3	4	5	6	7	8
39	409.2	674.6	773.4	877	1618.9	1195.5	1347.7	1420.8
40	409.1	674.2	772.8	876.8	1195.4	1347.6	1420.7	1471.4
41	408.9	674	772.4	876.4	1195.4	1347.4	1420.6	1471.3
42	408.8	673.9	772.1	876.1	1195.4	1347.3	1420.5	1471.2
43	408.7	673.5	771.6	875.9	1195.3	1347.1	1420.4	1471.1
44	408.6	673.4	771.4	875.6	1195.3	1347	1420.3	1471.1
45	408.5	673.3	771.1	875.4	1195.2	1346.9	1420.2	1470.9
46	408.5	673.3	771.1	875.4	1195.2	1346.9	1420.2	1470.9

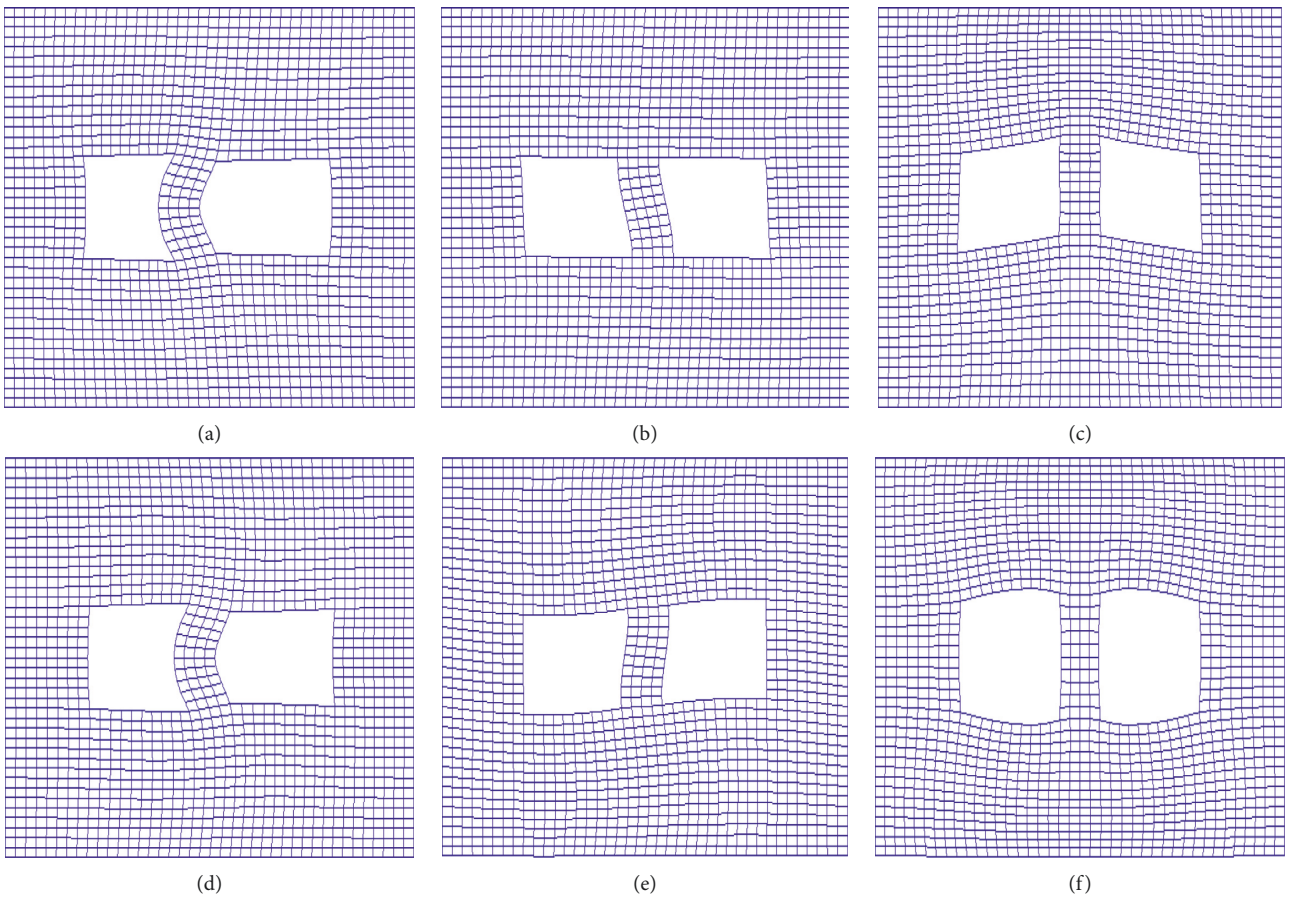

Figure 9: Mode shapes of in-plane vibration of the CCCC-FFFF-FFFF plate structure with two rectangular cutouts locating inside of the plate: the (a) first mode shape; (b) second mode shape; (c) third mode shape; (d) fourth mode shape; (e) fifth mode shape; and (f) sixth mode shape.

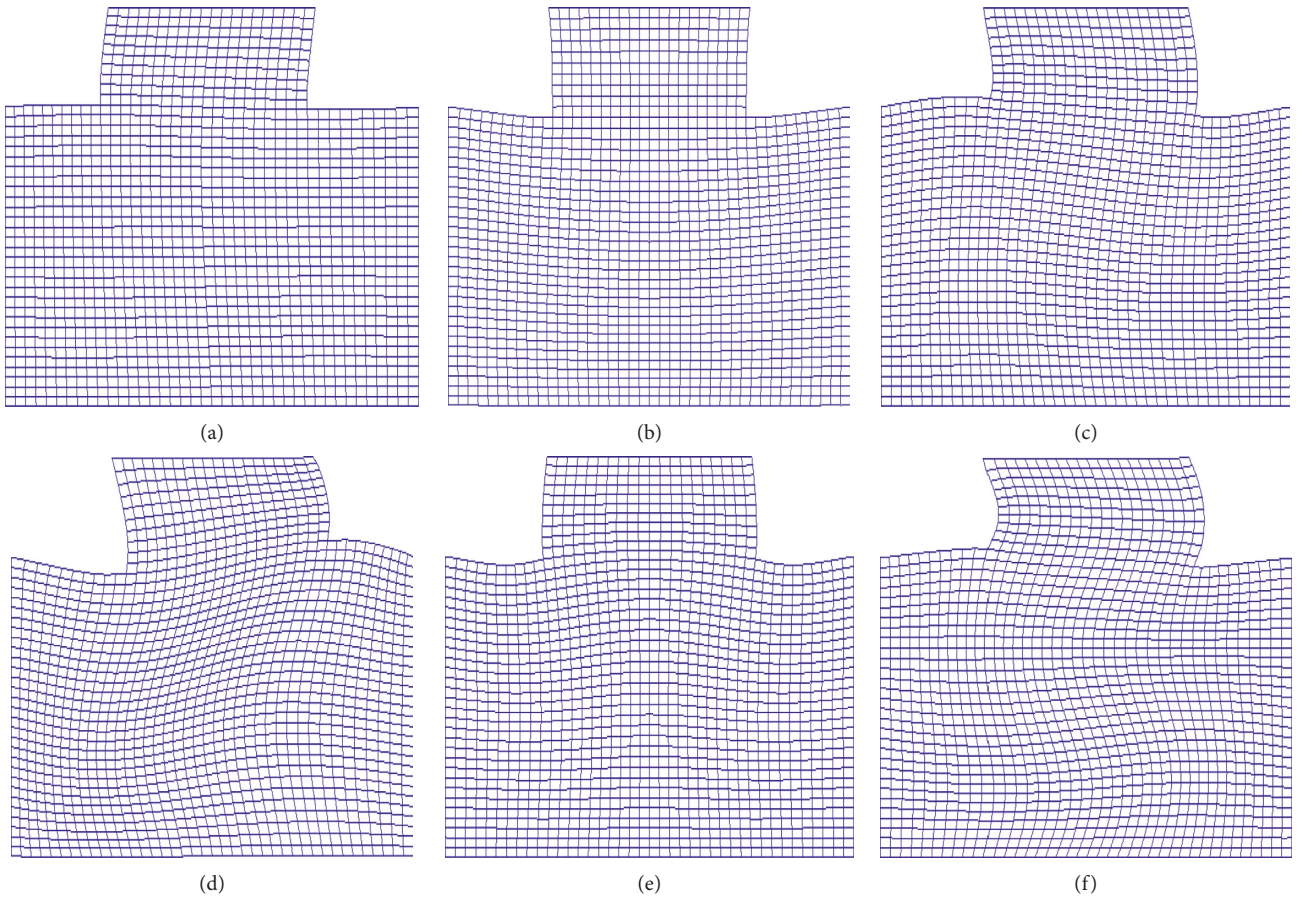

Figure 10: Mode shapes of in-plane vibration of the CCCC-FFFF plate structure with two rectangular cutouts locating on the corner of the plate: the (a) first mode shape; (b) second mode shape; (c) third mode shape; (d) fourth mode shape; (e) fifth mode shape; and (f) sixth mode shape.

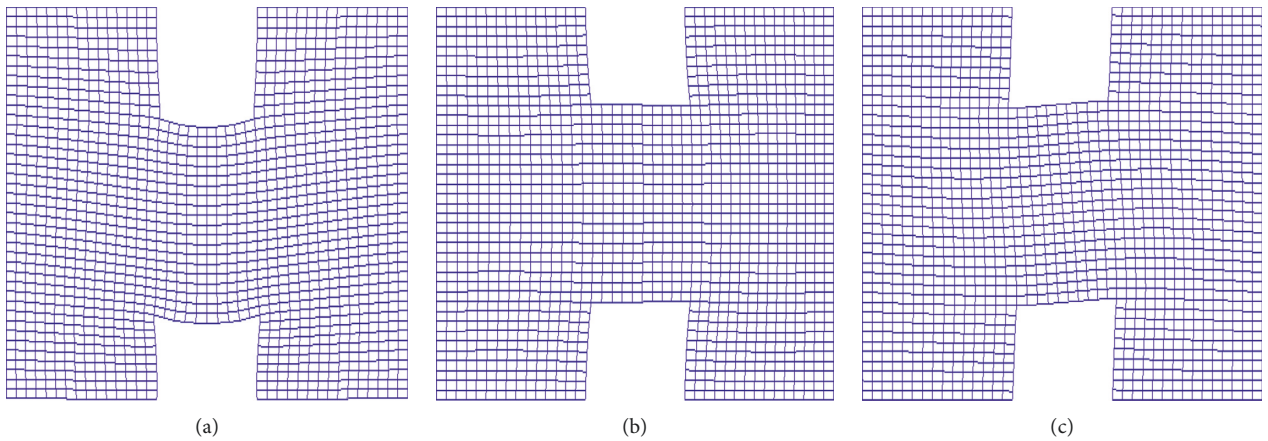

Figure 11: Continued.

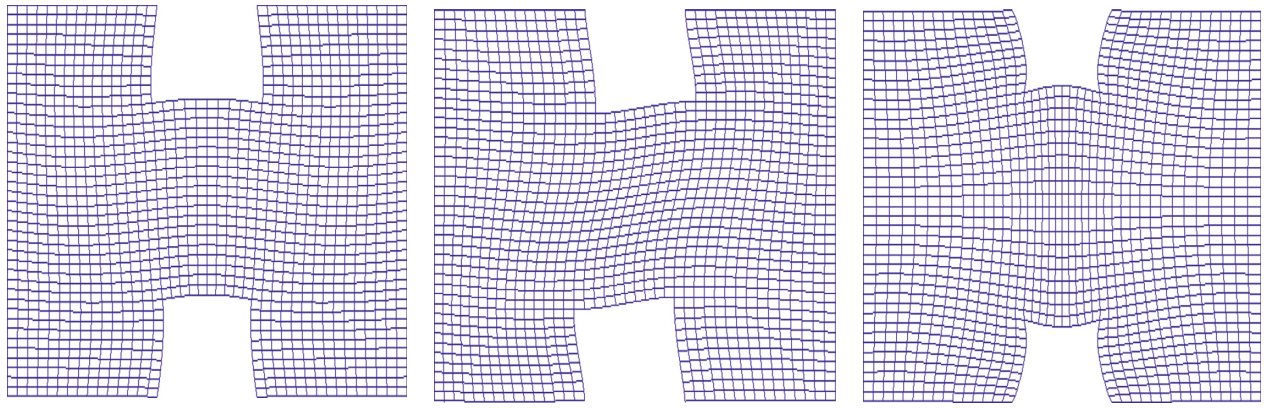

Figure 11: Mode shapes of in-plane vibration of the CCCCCC-FFFFFF plate structure with two rectangular cutouts locating on the boundary of the plate: the (a) first mode shape; (b) second mode shape; (c) third mode shape; (d) fourth mode shape; (e) fifth mode shape; and (f) sixth mode shape.

conditions. It can be clearly found that boundary conditions influence the vibration characteristics of the plate structure obviously. The first natural frequency of the same structure varies with different boundary conditions.

Next, the convergence of the current method for in-plane vibration will be studied. Structures considered here have the same geometric and material parameters as the plate with two cutouts defined in Section 3.1. Table 7 shows the frequency parameters of the FFFFFF-FFF-FFF plate with two edge rectangular cutouts determined by different truncated numbers. It can be found that as the truncated number increases the natural frequencies for in-plane vibrations change little at first, and when the truncated number is beyond 28, the natural frequencies remain unchanged. The desired convergence and numerical stability of the current method for in-plane vibration are validated.

As mentioned previously, the mode shapes of the plate with cutouts can be obtained by inserting the eigenvector into the displacement expressions. The first six mode shapes for in-plane vibration of the plate with two cutouts are shown in Figures 9–11, respectively. Compared with the flexural vibration of the plate with two cutouts, it can be found that not all mode shapes for in-plane vibration of the structure have symmetric characteristic.

4. Conclusions

A modified Fourier–Ritz formulation is presented for the flexural and in-plane vibration of plates with different kinds of cutouts (inner, edge, or corner). Under the current framework, the in-plane and flexural displacements of rectangular plates are expanded in the form of standard Fourier cosine series plus eight auxiliary polynomial functions. The current method is capable of universally dealing with cases with various positions of cutouts or different kinds of boundary restraint. The modification of the position or size of the cutouts is just like modifying the geometric parameters of the plate, and there is no need to change the solution procedure. The arbitrary elastic boundary conditions can be achieved by setting the stiffness constant of the boundary springs at proper values, for example, clamped boundary condition can be achieved by setting the stiffness constant of the boundary springs to infinite. Although, only uniform elastic restraints along the edge of the rectangular plate are studied in this paper, the modified Fourier–Ritz method can also be used for nonuniform elastic supports.

Several examples are presented in this paper to validate the desired accuracy and convergence of the current method. The effects of stiffness constants of the boundary springs on the solution results are also studied. It should be mentioned that with current method, the vibration of the plates with different kinds of cutouts or boundary conditions can be studied in a unified solution procedure. The vibration characteristics of the plate structure with rectangular cutouts are studied. The results show that both the position of cutouts and boundary conditions of the plate will influence the vibration characteristics of the structure obviously. The mode shapes for flexural and in-plane vibration of the plates with cutouts located inside of the plate or on the edge of the plate or on the corner of the plate are plotted in this paper.

Appendix

Detailed Expressions for the Elements in Mass Matrix and Stiffness Matrix

The detailed expressions of the stiffness and mass matrices in Equations (33) and (34) are given as follows: to make the expressions simple and clear, six indexes are predefined:

$$
\begin{aligned}
s &= m' \times (N+1) + (n'+1),\\
t &= m \times (N+1) + n + 1,\\
p &= (i-1) \times (M+1) + m + 1,\\
q &= (i-1) \times (N+1) + n + 1,\\
\{K_{11}\}_{s,t} &= \int_0^a \int_0^b [D_{11}\lambda_{am'}^2\lambda_{am}^2 \cos\lambda_{am'}x \cos\lambda_{am}x \cos\lambda_{bn'}y \cos\lambda_{bn}y + D_{22}\lambda_{bn'}^2\lambda_{bn}^2 \cos\lambda_{am'}x \cos\lambda_{am}x \cos\lambda_{bn'}y \cos\lambda_{bn}y\\
&\quad + D_{12}\lambda_{am'}^2\lambda_{bn}^2 \cos\lambda_{am'}x \cos\lambda_{am}x \cos\lambda_{bn'}y \cos\lambda_{bn}y + D_{21}\lambda_{am}^2\lambda_{bn'}^2 \cos\lambda_{am'}x \cos\lambda_{am}x \cos\lambda_{bn'}y \cos\lambda_{bn}y\\
&\quad + D_{66}\lambda_{am'}\lambda_{am}\lambda_{bn'}\lambda_{bn} \sin\lambda_{am'}x \sin\lambda_{am}x \sin\lambda_{bn'}y \sin\lambda_{bn}y]dx\,dy + \left[k_{ux0} + (-1)^{m+m'}k_{uxa}\right]\int_0^b \cos\lambda_{bn'}y \cos\lambda_{bn}y\,dy\\
&\quad + \left[k_{y0} + (-1)^{n+n'}k_{yb}\right]\int_0^a \cos\lambda_{am'}x \cos\lambda_{am}x\,dx,\\
\{K_{12}\}_{s,p} &= \sum_{i=1}^{4}\int_0^a \int_0^b [D_{11}\lambda_{am'}^2\lambda_{am}^2 \cos\lambda_{am'}x \cos\lambda_{am}x \cos\lambda_{bn'}y\zeta_{ib}(y) - D_{22}\lambda_{bn'}^2 \cos\lambda_{am'}x \cos\lambda_{am}x \cos\lambda_{bn'}y\zeta_{ib}''(y)\\
&\quad + D_{12}\lambda_{am'}^2\lambda_{bn}^2 \cos\lambda_{am'}x \cos\lambda_{am}x \cos\lambda_{bn'}y\zeta_{ib}(y) - D_{21}\lambda_{am}^2 \cos\lambda_{am'}x \cos\lambda_{am}x \cos\lambda_{bn'}y\zeta_{ib}''(y)\\
&\quad - D_{66}\lambda_{am'}\lambda_{am}\lambda_{bn'} \sin\lambda_{am'}x \sin\lambda_{am}x \sin\lambda_{bn'}y\zeta_{ib}'(y)]dx\,dy + \left[k_{ux0} + (-1)^{m+m'}k_{uxa}\right]\int_0^b \cos\lambda_{bn'}y\zeta_{ib}(y)dy\\
&\quad + \left[k_{uy0}\zeta_{ib}(0) + (-1)^{n+n'}\zeta_{ib}(b)\right]\int_0^a \cos\lambda_{am'}x \cos\lambda_{am}x\,dx,\\
\{K_{13}\}_{s,q} &= \sum_{i=1}^{4}\int_0^a \int_0^b [-D_{11}\lambda_{am'}^2\zeta_{ia}''(x)\cos\lambda_{am'}x \cos\lambda_{bn'}y \cos\lambda_{bn}y + D_{22}\lambda_{bn'}^2\lambda_{bn}^2 \cos\lambda_{am'}x\zeta_{ia}(x)\cos\lambda_{bn'}y \cos\lambda_{bn}y\\
&\quad + D_{12}\lambda_{am'}^2\lambda_{bn}^2 \cos\lambda_{am'}x\zeta_{ia}(x)\cos\lambda_{bn'}y \cos\lambda_{bn}y - D_{21}\lambda_{bn'}^2 \cos\lambda_{am'}x\zeta_{ia}''(x)\cos\lambda_{bn'}y \cos\lambda_{bn}y\\
&\quad - D_{66}\lambda_{am'}\lambda_{bn'}\lambda_{bn} \sin\lambda_{am'}x\zeta_{ia}'(x)\sin\lambda_{bn'}y \sin\lambda_{bn}y]dx\,dy + \left[k_{ux0}\zeta_{ia}(0) + (-1)^{m+m'}k_{uxa}\zeta_{ia}(a)\right]\int_0^b \cos\lambda_{bn'}y\zeta_{ib}(y)dy\\
&\quad + \left[k_{uy0} + (-1)^{n+n'}\right]\int_0^a \cos\lambda_{am'}x \cos\lambda_{am}x\,dx, \quad K_{14},\ldots,K_{19} = 0.
\end{aligned}
\tag{A.1}
$$

The other elements in stiffness matrix are similar to those derived previously.

$$
\begin{aligned}
\{M_{11}\}_{s,t} &= m\int_0^a \int_0^b \cos\lambda_{am'}x \cos\lambda_{am}x \cos\lambda_{bn'}y \cos\lambda_{bn}y\,dx\,dy,\\
\{M_{12}\}_{s,q} &= \sum_{i=1}^{4} m\int_0^a \int_0^b \cos\lambda_{am'}x\zeta_{ia}(x)\cos\lambda_{bn'}y \cos\lambda_{bn}y\,dx\,dy,\\
\{M_{13}\}_{s,p} &= \sum_{i=1}^{4} m\int_0^a \int_0^b \cos\lambda_{am'}x \cos\lambda_{am}x \cos\lambda_{bn'}y\zeta_{ib}(y)\,dx\,dy,\\
M_{14},\ldots,M_{19} &= 0.
\end{aligned}
\tag{A.2}
$$

The other elements in mass matrix are similar to those mentioned previously.

Data Availability

All relevant data are within the paper, and data sources are public.

Conflicts of Interest

The authors declare that there are no conflicts of interest regarding the publication of this paper.

Acknowledgments

This paper was supported by the National Natural Science Foundation of China (Nos. 51822902, 51775125, and 51279035) and the Fundamental Research Funds for the Central Universities of China (No. HEUCFG201713).

References

[1] A. N. Bercin, "An assessment of the effects of in-plane vibrations on the energy flow between coupled plates," *Journal of Sound and Vibration*, vol. 191, no. 5, pp. 661–680, 1996.

[2] A. W. Leissa, *Vibration of Plates*, Acoustical Society of America, Washington, DC, USA, 1993.

[3] C. Maury, P. Gardonio, and S. J. Elliott, "A wavenumber approach to modeling the response of a randomly excited

panel, part I: general theory," *Journal of Sound and Vibration*, vol. 252, no. 1, pp. 83–113, 2002.

[4] D. J. Gorman, *Vibration Analysis of Plates by the Superposition Method*, World Scientific Publishing, Singapore, 1999.

[5] D. J. Gorman, "A general solution for the free vibration of rectangular plates resting on uniform elastic edge supports," *Journal of Sound and Vibration*, vol. 139, no. 2, pp. 325–335, 1990.

[6] G. Y. Jin, T. G. Ye, X. R. Wang, and X. H. Miao, "A unified solution for the vibration analysis of FGM doubly-curved shells of revolution with arbitrary boundary conditions," *Composites Part B: Engineering*, vol. 89, pp. 230–252, 2016.

[7] H. C. Li, F. Z. Pang, X. R. Wang, and S. Li, "Benchmark solution for free vibration of moderately thick functionally graded sandwich sector plates on two-parameter elastic foundation with general boundary conditions," *Shock and Vibration*, vol. 2017, Article ID 4018629, 35 pages, 2017.

[8] Y. Mochida, "The boundedness of Gorman's superposition method for free vibration analysis of plates," *Computers Structures*, vol. 104-105, pp. 38–43, 2012.

[9] W. L. Li, "Free vibrations of beams with general boundary conditions," *Journal of Sound and Vibration*, vol. 237, no. 4, pp. 709–725, 2000.

[10] P. A. A. Laura and R. H. Gutierrez, "Analysis of vibrating rectangular plates with non-uniform boundary conditions by using the differential quadrature method," *Journal of Sound and Vibration*, vol. 173, no. 5, pp. 702–706, 1994.

[11] C. Shu and H. Du, "A generalized approach for implementing general boundary conditions in the GDQ free vibration analysis of plates," *International Journal of Solids and Structures*, vol. 34, no. 7, pp. 837–846, 1997.

[12] X. Wang, L. Gan, and Y. Wang, "A differential quadrature analysis of vibration and buckling of an SS-C-SS-C rectangular plate loaded by linearly varying in-plane stresses," *Journal of Sound and Vibration*, vol. 298, no. 1-2, pp. 420–431, 2006.

[13] D. J. Gorman, "Free in-plane vibration analysis of rectangular plates with elastic support normal to the boundaries," *Journal of Sound and Vibration*, vol. 285, no. 4-5, pp. 941–966, 2005.

[14] D. J. Gorman, "Free in-plane vibration analysis of rectangular plates by the method of superposition," *Journal of Sound and Vibration*, vol. 272, no. 3–5, pp. 831–851, 2004.

[15] Q. Wang, D. Shi, Q. Liang, and F. E. Ahad, "A unified solution for free in-plane vibration of orthotropic sector, annular and circular plates with general boundary conditions," *Applied Mathematical Modelling*, vol. 40, no. 21-22, pp. 9228–9253, 2016.

[16] Z. Y. Shi, X. L. Yao, F. Z. Pang, and Q. S. Wang, "A semi-analytical solution for in-plane free vibration analysis of functionally graded carbon nanotube reinforced composite circular arches with elastic restraints," *Composite Structures*, vol. 182, pp. 420–434, 2017.

[17] N. H. Farag and J. Pan, "Free and forced in-plane vibration of rectangular plates," *Journal of the Acoustical Society of America*, vol. 103, no. 1, pp. 408–413, 1998.

[18] N. H. Farag and J. Pan, "Modal characteristics of in-plane vibration of rectangular plates," *Journal of the Acoustical Society of America*, vol. 105, no. 6, pp. 3295–3310, 1999.

[19] Y. F. Xing and B. Liu, "Exact solutions for the free in-plane vibrations of rectangular plates," *International Journal of Mechanical Sciences*, vol. 51, no. 3, pp. 246–255, 2009.

[20] Y. S. Zhou, Q. S. Wang, D. Y. Shi, Q. Liang, and Z. Zhang, "Exact solutions for the free in-plane vibrations of rectangular plates with arbitrary boundary conditions," *International Journal of Mechanical Sciences*, vol. 130, pp. 1–10, 2017.

[21] M. Huang and T. Sakiyama, "Free vibration analysis of rectangular plates with variously shaped holes," *Journal of Sound and Vibration*, vol. 226, no. 4, pp. 769–786, 1999.

[22] M. K. Kwaka and S. Han, "Free vibration analysis of rectangular plate with a hole by means of independent coordinate coupling method," *Journal of Sound and Vibration*, vol. 306, no. 1-2, pp. 12–30, 2007.

[23] P. A. A. Laura, E. Romanelli, and R. E. Rossi, "Transverse vibrations of simply supported rectangular plates with rectangular cutouts," *Journal of Sound and Vibration*, vol. 202, no. 2, pp. 275–283, 1997.

[24] D. R. Avalos and P. A. A. Laura, "Transverse vibrations of simple supported rectangular plates with two rectangular cutouts," *Journal of Sound and Vibration*, vol. 267, no. 4, pp. 967–977, 2003.

[25] I. Shufrin and M. Eisenberger, "In-plane vibrations of rectangular plates with rectangular cutouts," in *Proceedings of Computational Methods in Enginnering and Science, EPMSC X*, pp. 1185–1192, Sanya, Hainan, China, 2006.

[26] Y. H. Chen, G. Y. Jin, and Z. G. Liu, "Flexural and in-plane vibration analysis of elastically restrained thin rectangular plate with cutout using Chebyshev-Lagrangian method," *International Journal of Mechanical Sciences*, vol. 89, pp. 264–278, 2014.

[27] W. L. Li, "Comparison of Fourier sine and cosine series expansions for beams with arbitrary boundary conditions," *Journal of Sound and Vibration*, vol. 255, no. 1, pp. 185–194, 2002.

[28] G. Y. Jin, X. L. Ma, S. X. Shi, T. G. Ye, and Z. G. Liu, "A modified Fourier series solution for vibration analysis of truncated conical shells with general boundary conditions," *Applied Acoustics*, vol. 85, pp. 82–96, 2014.

[29] G. Y. Jin, Z. Su, T. G. Ye, and X. Z. Jia, "Three-dimensional vibration analysis of isotropic and orthotropic conical shells with elastic boundary restraints," *International Journal of Mechanical Sciences*, vol. 89, pp. 207–221, 2014.

[30] T. G. Ye, G. Y. Jin, and Z. Su, "Three-dimensional vibration analysis of laminated functionally graded spherical shells with general boundary conditions," *Composite Structures*, vol. 116, pp. 571–588, 2014.

[31] G. Y. Jin, T. G. Ye, X. L. Ma, Y. H. Chen, Z. Su, and X. Xie, "A unified approach for the vibration analysis of moderately thick composite laminated cylindrical shells with arbitrary boundary conditions," *International Journal of Mechanical Sciences*, vol. 75, pp. 357–376, 2013.

[32] Y. Q. Xue, G. Y. Jin, H. Ding, and M. F. Chen, "Free vibration analysis of in-plane functionally graded plates using a refined plate theory and isogeometric approach," *Composite Structures*, vol. 192, pp. 192–205, 2018.

[33] Z. Su, G. Jin, and T. Ye, "Electro-mechanical vibration characteristics of functionally graded piezoelectric plates with general boundary conditions," *International Journal of Mechanical Sciences*, vol. 138-139, pp. 42–53, 2018.